https://doi.org/10.5194/acp-2023-37
Preprint. Discussion started: 7 February 2023

Atmospheric Chemistry and Physics Discussions

Impact of the Atmospheric Boundary Layer Height on the Concentration of Chemical Species in Numerical Model Simulations

Shuzhan Ren[1] and Craig A Stroud[1]

[1]Air Quality Research Division, Science and Technology Branch, , Environment and Climate Change Canada, Toronto, Ontario, Canada

Correspondence: Shuhan Ren (shuzhan.ren@canada.ca)

Abstract.

The top of the atmospheric boundary layer (ABL) serves as a boundary separating turbulent air in the ABL and free atmosphere in the troposphere. The increase/decrease of the ABL height (ABL-H) can dilute or concentrate chemical species in the ABL. In numerical simulations the ABL-H is involved in computing the vertical diffusivity and the counter-gradient term under the unstable condition in ABL parameterization schemes. Therefore, uncertainties in the ABL-H due to the uncertainties in meteorological fields and different definitions can affect the numerical predictions of the concentration of chemical species. To understand the impacts, a 1-D diffusion model with the K-profile scheme and an 3-D air quality forecast model with the turbulent kinetic energy (TKE)-based scheme are employed to examine the sensitivities of diffusion coefficient, counter-gradient term and tracer's concentration to the ABL-H analytically and numerically. Sensitivity tests with the 1-D model show that the increase/decrease of the ABL-H leads to the decrease/increase of concentration of tracers under both stable and unstable conditions due to the increase/decrease of the volume of air within the ABL. Under the unstable condition, the increase/decrease of the ABL-H also enhances/weakens the vertical diffusivity, and leads to the decrease/increase of the concentration of tracers for negative/positive vertical gradient of tracer. The impact of the ABL-H through the counter-gradient term is much smaller than the impact through changing the volume of trace and vertical diffusivity in the ABL. Sensitivity tests with the 3-D numerical model with the TKE scheme show increase/decrease of the ABL-H leads to strong/weak vertical diffusivity, but has very small impact of the ABL-H on the concentrations of pollutants over urban centers for the ABL-Hs which is defined based on the Richardson number and temperature.

1 Introduction

The atmospheric boundary height (ABL-H) is a parameter describing the vertical extent of turbulent mixing. The inversion layers at the top of the ABL serve as a capping lid, and its evolution can dilute or enhance the concentration of chemical species within the ABL. Therefore, the ABL-H has a great impact not only on the transport of heat and momentum but also on the transport and dispersal of chemical species within the ABL.

Culf et al. (1997) investigated the influence of the ABL on the averaged CO2 concentration within the ABL over the tropical forecast. By analysing the results of a simple 1-D bulk model and observations they found that while daytime CO_2 mean

https://doi.org/10.5194/acp-2023-37
Preprint. Discussion started: 7 February 2023

Atmospheric Chemistry and Physics Discussions

concentration is controlled almost entirely by mixed layer growth, with the surface flux playing a very small role, nocturnal CO_2 mean concentrations are much more sensitive to differences in both boundary layer height and surface flux of CO2. However, the work of Arellano et al. (2004)shows that the mixed layer growth is more important in affecting averaged CO_2 concentration than the surface uptake only in the morning. The surface uptake becomes dominant in other time.

The relationship between the ABL-H and the concentration of air pollutants has been widely investigated. Su et al. (2018,2020) examined the role of the ABL-H in pollution events. Their results show that there is a negative correlation between the ABL-H and near surface air pollutants. The shallow ABL can lead to severe air pollution episodes even when the anthoropogenic emissions were significantly reduced during the lockdown due to the Covid-19 pandemic in 2020. Long term observations suggest the negative correlation between the ABL-H and diffusion capacity of air pollutants (Xiang et al., 2019; Lee et al., 2019).

The 1-D bulk model is a useful tool for understanding the relationship. It has been employed by Raupach (1991), Denmead et al. (1996), Culf et al. (1997), Dang et al. (2011) and Pino et al. (2012) to examine the impacts of the ABL-H, surface flux, and entrainment on the mean CO_2 concentration (defined as the vertically integrated mixing ratio from ground to the top of ABL divided by the ABL-H). The results of Pino et al. show analytically the dependence of the mean concentration on the ABL-H under the fluxes from upper and lower boundaries. If the flux from the upper boundary is very small, the mean CO_2 concentration is inversely proportional to the ABL-H. Ren (2019) derived an analytical solution to the 1-D diffusion model with height-independent diffusion coefficient. The solution shows that the increase of the ABL-H leads to exponential decrease of concentration of tracers.

The evolution of the ABL-H is driven by many factors including surface heat flux, weather patterns, advection of meteorological fields, surface roughness and land coverage etc. (e.g., Tennekes, 1973; Culf, 1991). In numerical models, The ABL-H is a diagnostic variable whose value is determined mostly by the potential temperature profile or Richardson number. It has long been recognized that there are big uncertainties in the ABL-H. These uncertainties are associated with not only the uncertainties in meteorological variables involving in the definition of the ABL-H, such as temperatures, winds and humidity but also different definitions of ABL-H. The work of Seidel et al. (2010, 2012) shows that the uncertainties in meteorological fields can produce more than 50% uncertainty in shallow boundary layers and 20% in deeper boundary layers. In addition, ABL-H with different definitions can have very different values even under the same meteorological conditions (e.g., Ren et al., 2020).

Because the ABL-H is involved in ABL parameterization schemes employed by numerical models, it can affect chemical species not only by diluting or concentrating chemical species within the ABL, but also by impacting on vertical diffusivity and the counter-gradient term through the convective velocity. Thus, in additional to the direct impacts on the transport of chemical species, uncertainties in meteorologicla variables can further impact the model simulations of chemical species indirectly through the ABL-H. Given the large uncertainties in the ABL-H associated with the uncertainties of meteorological variables and the ABL-H definitions, its impacts on the concentration of chemical species in numerical model simulations should be examined. Understanding the impacts can help understand the different chemical species simulated with different ABL-H definition or with the same ABL-H definition but different numerical models. More importantly, it can help quantify the uncertainties in air quality simulations associated with the ABL-H uncertainties.

https://doi.org/10.5194/acp-2023-37
Preprint. Discussion started: 7 February 2023


Atmospheric Chemistry and Physics Discussions

In previous studies based on the 1-D bulk model, only the averaged concentration is considered, and it cannot describe the impact on the concentration at different height due to the lack of detailed description of turbulent mixing. The analytical solution derived by Ren (2019) is based on the height-independent diffusion coefficient assumption, it can only provide a qualitative description of the impact of the ABL-H. In this work, the K-profile and turbulent kinetic energy (TKE)-based parameterization schemes are employed to understand how the uncertainties in the ABL-H affect chemical species. In this work, a 1-D diffusion model with the K-profile scheme is used first to show the sensitivity of tracer's concentration to the ABL. A 3-D air quality forecast model– Global Environmental Multiscale Model-Modelling Air Quality and Chemistry (GEM-MACH) is then used to investigate the impacts of the ABL on the forecasts of concentration of chemical species.

This paper is organized as follows. A 1-D model with the K-profile parameterization scheme is employed in section 2 to examine the impacts the ABL-H on vertical diffusivity, counter-gradient term, and tracer's concentration. In section 3, the role of the ABL-H in the TKE-based parameterization scheme is discussed, and the sensitivities of concentration of chemical species to the ABL-H are investigated with GEM-MACH. Summary and discussion are given in the last section.

2 Impacts of ABL-H in the K-profile parameterization scheme

The ABL parameterization schemes have been widely employed in ABL dynamics and numerical models to describe the turbulence contributions to the motions within the ABL. In the schemes, diffusion coefficient and the ABL-H are two important parameters, and they are correlated positively under the unstable condition due to their association with the surface heat flux. The relationship of the two parameters is described differently in different parameterization schemes. The ABL-H can be also involved in the parameterization of the surface drag coefficient (e.g., Lorentz-Plazas et al. 2016). Therefore, the ABL-H in the numerical simulations can have impacts on the dynamics of the ABL as well as the transport of chemical tracers. In this work only the impacts on chemical tracers through the counter-gradient term and diffusion coefficients are discussed. In this part, the impacts of the ABL-H in the K-profile parameterization scheme on counter-gradient term, vertical diffusivity, and tracer's concentration analytically and numerically.

2.1 Impact on the counter-gradient term

In ABL parameterization schemes, the turbulent flux of a scalar variable ψ is parameterized as

$$\overline{w'\psi'} = -K\left(\frac{\partial \psi}{\partial z} - \gamma_\psi\right), \tag{2.1}$$

where K is the eddy vertical diffusion coefficient. The counter-gradient term γ_ψ is used to describe the nonlocal transport associated with large-eddy motions in a convective boundary which is defined as (Holtslag and Moeng, 1991)

$$\gamma_\psi = a\frac{w_*\overline{\psi'w'}|_s}{hw_m^2}, \tag{2.2}$$

https://doi.org/10.5194/acp-2023-37
Preprint. Discussion started: 7 February 2023

Atmospheric Chemistry and Physics Discussions

where a is a constant (7$\sim$ 10), $w_m = (u_*^3 + c_1 w_*^3)^{1/3}$, c_1 is a constant, u_* is the friction velocity, w_* is the convective velocity defined as

$$w_*^3 = hB_0 \equiv \frac{gh\overline{\theta' w'}|_s}{\theta_{vs}}, \tag{2.3}$$

h is the ABL-H. Because $B_0 \sim 1.4 \times 10^{-2}$ m^2 s^{-3} (corresponding to heat flux ($\rho C_p \overline{\theta' w'}|_s$) of 500 W m^{-2}) at midday, $w_* \sim 14^{1/3} \sim 2.4$ m s^{-1} for the ABL-H of 1000 m. Note that w_* is set to zero for negative (downward) surface heat flux.

Since $w_* h = B_0^{1/3} h^{4/3}$, γ_ψ is proportional to $h^{-4/3}$ in very unstable case ($w_* >> u_*$). Thus, the corresponding changes of w^* and γ_ψ to the change of h are

$$\frac{\delta w^*}{w^*} = \frac{1}{3}\frac{\delta h}{h}, \quad \frac{\delta \gamma_\psi}{\gamma_\psi} = -\frac{4}{3}\frac{\delta h}{h}. \tag{2.4}$$

To examine The impact of the ABL-H on γ_ψ numerically, the fluxes shown in Fig.1 are used. Fig.1a represents the biogenic CO_2 flux Ren (2019) with upward flux in the early morning and night time due to respiration, and downward flux during the daytime due to photosynthesis of CO_2. Figure 1b shows the flux from industrial activities. In the sensitivity tests, the evolution of the ABL-H is prescribed by

$$h = \begin{cases} hf * 100 + (hf * 1000 - 100)\cos\left(\frac{t-12}{12}\pi\right) & 6hr < t < 18hr \\ hf * 100 & 6hr \geq t \geq 0, \quad t \geq 18hr. \end{cases} \tag{2.5}$$

where hf is a factor for sensitivity test, and $hf = 1$ for the benchmark case, $hf * 1000$ m is the maximum ABL-H at $t = 12$. The ABL is assumed to be unstable between 6:00AM and 6:00PM, and the convective vertical velocity w_* is computed using $w_*^3 = 0.015h\cos(t-12)\pi/12)$, and $\gamma_\psi = 7.5 w_* F/(h w_m^2)$, where $w_m = (0.3^3 + w_*^3)^{1/3}$ and F is the surface flux shown in Fig. 1. They are zero at other times. The diurnal variations of w_* and γ_ψ are shown in Figure 2a and 2b, respectively, with $H = 1$ km and with the first kind of surface flux scheme.

To show the sensitivity of w_* and γ_ψ to the ABL-H, their values with $hf = 1.1, 1.2, 1.3, 1.4$ are computed and the differences between these values and the benchmark values with $hf = 1.0$ are shown in Fig.2c and fig.2d, respectively. It can be seen from Fig.2c that the increase of the ABL-H leads to the increase of w_* and the maximum differences occur at midday when the ABL-H reaches to maximum. The changes of w^* corresponding to the change of the ABL-H roughly agree with Eq. (2.4). For example, for hf =1.4, the difference at midday shown in Fig.2c is about 0.3 and is about 0.33 ($w^* \delta h/3h$) according to Eq. (2.4). Figure 2d shows that due to the negative surface flux, γ_ψ is negative between 6:00AM to 8:00PM, the increase of the ABL-H leads to the increase of γ_ψ, and the maximum differences appear at around 8:00AM.

2.2 Impact on the diffusion coefficient

Under the unstable condition (mostly during the daytime), the diffusion coefficient in the K-profile closure scheme proposed by Holtslag and Boville (1993) is

https://doi.org/10.5194/acp-2023-37
Preprint. Discussion started: 7 February 2023

Atmospheric Chemistry and Physics Discussions

$$K = kw_t z\left(1-\frac{z}{h}\right)^2, \tag{2.6}$$

where k is the Karman constant, $w_t = u_*/\phi_M$ for the stable boundary layer, ϕ_M is the dimensionless vertical temperature gradient, $w_t = w_m/Pr$ for the unstable boundary layer, Pr is the Prandtl number. Because w_t contains the ABL-H, the dependence of K on h is highly nonlinear, and the increase of the ABL-H leads to the increase of K.

In the K-profile parameterization scheme, the ABL-H is involved explicitly in computing the diffusion coefficient under the unstable condition. At the top of the ABL, diffusivity vanishes regardless of the definition of the ABL-H. It will be seen that this is not the case in the TKE-based scheme.

It should be pointed out that although both surface heat flux and the ABL-H contained in w^* can affect K, their impacts are different. The change of former can lead to the change of the ABL-H and further change of K. Furthermore, the change of surface heat flux may lead to the change of stability condition and consequently change K.

At midday, $h \sim 1000$ m, $u_* << w_*$. Therefore, at the low ABL ($z << h$), the corresponding change of K to the change of h is

$$\frac{\delta K}{K} \sim \frac{\delta h}{3h}. \tag{2.7}$$

For a 30% change of $\delta h/h$, $\delta K/K$ is about 10%.

The diffusion coefficients at 30 m and 200 m with $hf = 1$ are shown in Fig. 3a and 3b, respectively. Between 6:00AM to 18:00PM the diffusion coefficient is computed using Eq. (2.5) and is 2 m^2 s^{-1} in other time. The differences between them and those with hf =1.1, 1.2, 1.3, 1.4 are shown in Fig. 3c and 3d, respectively. As with the impact on w^*, the increase of the ABL-H leads to the increase of diffusion coefficient. The differences between K_T with $hf = 1$ and those with hf =1.1, 1.2, 1.3, 1.4 are roughly close to the difference estimated by Eq. (2.6). At $z = 30$ m, the difference at midday is about 3.25 m^2 s^{-1} for hf =1.4 in Fig. 3c and is about 3.33 m^2 s^{-1} according to Eq. (2.7).

2.3 Impact on the concentration of tracer

Because the ABL-H involves in the calculation of the vertical diffusion coefficient in Eq. (2.6), the change of the diffusivity associated with the change of the ABL-H shown above would lead to the change of concentration of tracers. To illustrate the impacts on tracer's concentration, the following 1-D diffusion model

$$\frac{\partial \psi}{\partial t} = \frac{\partial}{\partial z}\left(K\frac{\partial \psi}{\partial z}\right) \tag{2.8}$$

is used. The work of Ren (2019) shows that this simple model can describe the important features of CO_2 evolution even with a simple time-dependent diffusion coefficient.

Two kinds of surface flux of tracer shown in Fig. 1 are used in the lower boundary condition for Eq. (2.8). For simplicity, zero flux at the top of the ABL is used. The initial condition of ψ (ppmv) below the top of the ABL used in the computations is.

https://doi.org/10.5194/acp-2023-37
Preprint. Discussion started: 7 February 2023

Atmospheric Chemistry and Physics Discussions

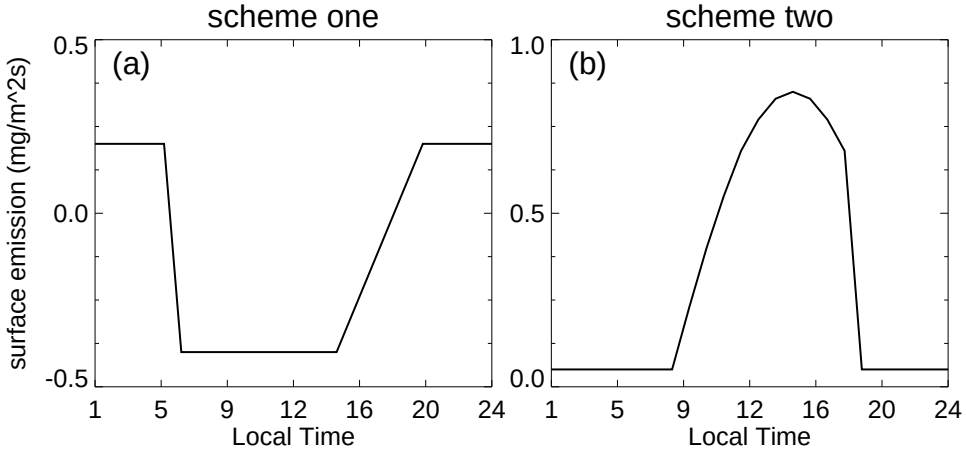

Figure 1. Diurnal variation of two kinds of surface flux.

$$\psi(z, t = 0) = 420 - 0.03\alpha z, \tag{2.9}$$

where α is a (positive) constant measuring the vertical gradient of initial condition.

The corresponding change of tracer's concentration to the change of the diffusion coefficient can be described by the following equation (Ren and Stroud, 2020)

$$\delta\psi = -\int_0^t \int_0^h \frac{\partial\psi}{\partial z'} \frac{\partial G}{\partial z'} \Delta K dz' d\tau, \tag{2.10}$$

where ψ is the benchmark mixing ratio with $hf = 1$, ΔK is the change of diffusion coefficient, G is the Green's function (Ren and Stroud, 2020). Equation (2.10) is derived based on a 1-D model but can be generalized in the 3-D case. The work of Ren and Stroud (2020) shows that in the 1-D model with the height-independent diffusion coefficients the gradient of G is negative near the ground. Thus Eq. (2.10) suggests that in the 1-D model the increase/decrease of K would lead to decrease/increase of ψ for negative $\partial\psi/\partial z$ and increase/decrease of ψ for positive $\partial\psi/\partial z$. This is important for understanding the following numerical results based on the 1-D diffusion model.

https://doi.org/10.5194/acp-2023-37
Preprint. Discussion started: 7 February 2023

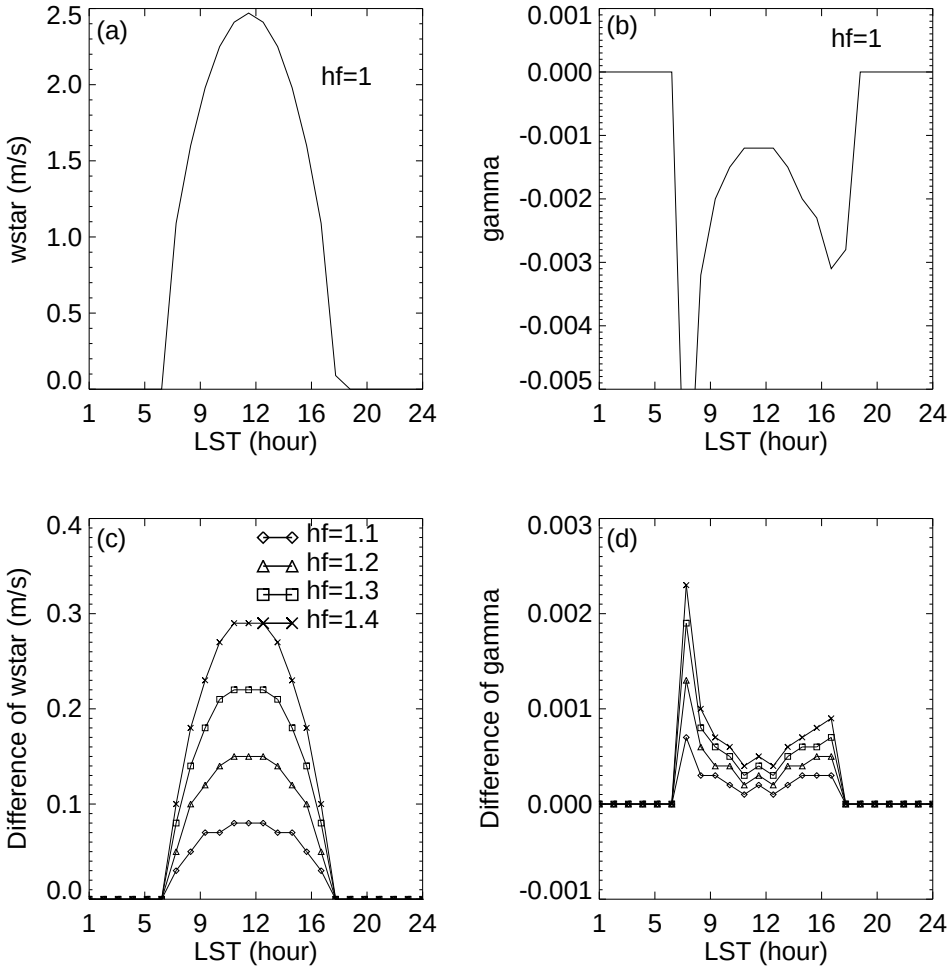

Figure 2. Diurnal variation of convective velocity w_* (a) and counter-gradientγ_ψ (b) with the first kind of surface flux and with hf =1.0. The differences between w_* with hf =1 and w_* with hf =1.1, 1.2, 1.3, 1.4 are shown in (c), and the differences between γ_ψ with hf =1 and γ_ψ with hf =1.1, 1.2, 1.3, 1.4 are shown in (d).

https://doi.org/10.5194/acp-2023-37
Preprint. Discussion started: 7 February 2023

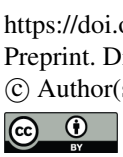

Atmospheric Chemistry and Physics Discussions

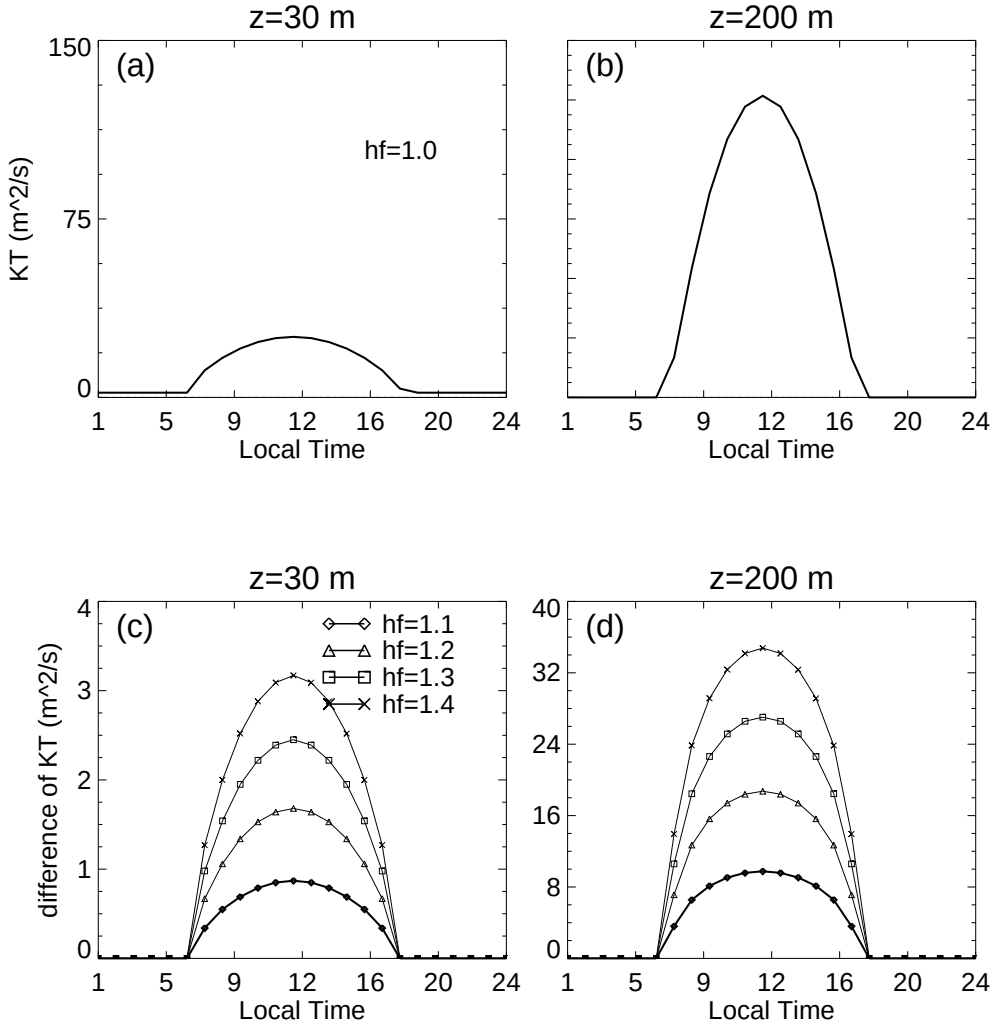

Figure 3. Diurnal variation of diffusion coefficient K with hf =1 at 30 m (a) and at 200 m (b). The differences between K with hf =1.1, 1.2, 1.3, 1.4 and the benchmark K at 30 m and 200 m are shown in (c) and (d), respectively.

In order to examine the impact of the ABL-H, ψ with hf =1 and $\gamma_\psi = 0$ is used as the benchmark results. The benchmark mixing ratios for different gradient factor (α) are computed with the two surface flux. Figures. 4 and 5 show the diurnal

https://doi.org/10.5194/acp-2023-37
Preprint. Discussion started: 7 February 2023


Atmospheric Chemistry and Physics Discussions

variation of the departure of the mixing ratio from 420 ppmv at 30 m for the first and second kind of surface flux, respectively. Due to the diurnal variation of vertical diffusivity, the diurnal variations in both Fig.4 and Fig. 5 show the strong rectifier effect with a big jump of mixing ratio around 6:00AM and then a quick drop afterwards. The drop lasts longer in Fig.4 than in Fig. 5 due to the negative surface flux during the daytime. The figures also show that large gradient factor leads to a big reduction of mixing ratio.

The uncertainties in the ABL-H cause the change not only in the vertical diffusivity but also in the volume of tracer in the ABL. Both factors contribute to the sensitivity of mixing ratio shown in the following numerical results. To examine the sensitivity of ψ to the ABL-H, hf =0.6, 0.8, 1.3, 1.4 are used to represent four scenarios with under- and over-estimated ABL-H.

Figure 6 shows the mixing ratio differences between the four scenario results and the benchmark results at 30 m for different gradient factor with the first kind surface flux. It can be seen from the figure that in the early morning and nighttime increase/decrease of the ABL-H leads to decrease/increase of mixing ratio. Because diffusivity does not change with the ABL-H during this period, the change of mixing ratio is entirely due to the change of the volume of tracer in the ABL and is not sensitiv to the gradient factor. Comparison between Fig. 4 and Fig. 6 suggests that for $hf = 0.6$ and $hf = 1.4$, the increase and decrease of mixing ratio can be 60% and 20%, respectively.

During daytime, the impact of the ABL-H on mixing ratio is sensitive to the gradient factor. For $\alpha = 0$, increase/decrease leads to the increase/decrease of mixing ratio. For large α, however, the sensitivity changes: the increase/increase of the ABL-H leads to the reduction/enhancement of mixing ratio after 6:00AM. The comparison between Fig. 6 and Fig. 4 shows that the reduction can be 20% of the mixing ratio in Fig.4 for α =1 and hf =1.4.

Although the vertical gradient of mixing ratio is negative (or zero for $\alpha = 0$) in the initial condition, it becomes positive after 6:00AM due to negative surface flux. Thus the increase/decrease of the ABL-H leads to the increase/decrease of mixing ratio by enhancing/reducing the vertical diffusivity (Eq. (2.9)), and at the same time leads to the decrease/increase of mixing ratio through diluting/concentrating. The results suggest that the former effect is dominant for small α (corresponding to large positive vertical gradient of tracer) and the latter effect is dominant for large α as shown in Fig. 6.

Because the second kind of surface flux is always positive, the vertical gradient of mixing ratio is always negative. Figure 7 shows that the increase/decrease of the ABL-H leads to the decrease/increase of mixing ratio all day regardless of the value of α. The increase of the ABL-H leads to the decrease of mixing ratio by enhancing the vertical mixing and the dilution effect, and the decrease of the ABL-H leads to increase of mixing ratio by weakening the vertical mixing and the concentration effect. The reduction/enhancement can be more than 100% of mixing ratio shown in Fig.5.

The impacts of the ABL-H on mixing ratio through γ_ψ can be assessed by comparing the numerical results with and without the counter-gradient included. Figure 8 shows such differences at 30 m with different ABL-H and the first kind of surface flux. The diurnal variation pattern shown in the figure is quite similar to that of γ_ψ difference (shown in Fig. 2d). Large ABL-H leads to the increase of mixing ratio, and the magnitude of the increase is much less than that of differences shown in Fig. 6, particularly for large gradient factor. The figure also suggests that the impacts are not so sensitive to the gradient factor.

https://doi.org/10.5194/acp-2023-37
Preprint. Discussion started: 7 February 2023

Atmospheric Chemistry and Physics Discussions

Under the second kind of surface fluxes the increase of the ABL-H leads to the decrease of mixing ratio after 6:00AM (Fig. 9). The magnitude of the decrease is also much smaller than the magnitude of mixing ratio difference shown in Fig. 7, and it is not sensitivey to the ABL-H before 6:00AM but sensitive afterwards. Like the case with the first kind of surface emission scheme, the mixing ratio differences are not sensitive to the gradient factor.

The above numerical results show that under the stable condition, the ABL-H affects the tracer's concentration by changing the volume of tracer in the ABL. Under the unstable condition, the ABL-H also affects tracer's concentration by changing the vertical diffusivity. This impact depends on both surface flux and the vertical gradient of tracers.

3 Impacts of the ABL-H in the TKE parameterization scheme

3.1 The ABL-H in the TKE-based scheme

The TKE scheme is another ABL parameterization scheme widely used in numerical models (Mailhot & Benoit, 1982, Benoit at al., 1989, Belair et al., 1999). The evolution of TKE is described by the following equation

$$\frac{\partial E}{\partial t} = BE^{1/2} - CE^{3/2} + \frac{\partial}{\partial z}\left(K_M \frac{\partial E}{\partial z}\right), \tag{3.1}$$

where B can be positive or negative depending on the local Richardson number, and C is always positive. Lower boundary condition for the equation is

$$E(z=0,t) = \begin{cases} 3.75u_*^2 & \text{stable} \\ 3.75u_*^2 + 0.2w_*^2 & \text{unstable} \end{cases} \tag{3.2}$$

Once TKE is available, the diffusion coefficient for momentum K_M is obtained from the following equation

$$K_M = \frac{c\lambda\sqrt{E}}{\phi_M}, \tag{3.3}$$

where $c = 0.516$, $\lambda = min[k(z+z_0), 200]$ is Blackadar's mixing length, z_0 is the roughness length.

Unlike the K-profile scheme in which the relationship between K and ABL-H can be described analytically and K is zero at the top of the ABL, the connection between $K_T(= K_M/Pr)$ and ABL-H in the TKE scheme cannot be explicitly described, and K_T does not vanish at the top of the ABL. This can be seen from Fig. 10 which shows the diurnal variation of K_T at the top of the ABL defined based on the vertical gradient of temperature (Fig. 10a) and Richardson number (Fig. 10b) over the urban center of Toronto. In the figure K_T is quite large between 5:00PM to 8:00PM for the two ABL-H definitions and between 10:00PM to 0:00 AM for the Richardson number based definition. It is also relatively large in other time. The large K_T shows the inconsistency between the zero diffusivity at the ABL top assumption and the definition of the ABL.

Because the ABL-H is contained in w_* it can affect the vertical diffusivity indirectly through the lower boundary condition for the TKE equation. This is very different from the way that the ABL-H affects the vertical diffusivity in the K-profile scheme in which the ABL-H involves in the diffusion coefficient explicitly within the ABL. Because the ABL-H affects E only under

https://doi.org/10.5194/acp-2023-37
Preprint. Discussion started: 7 February 2023

Atmospheric Chemistry and Physics Discussions

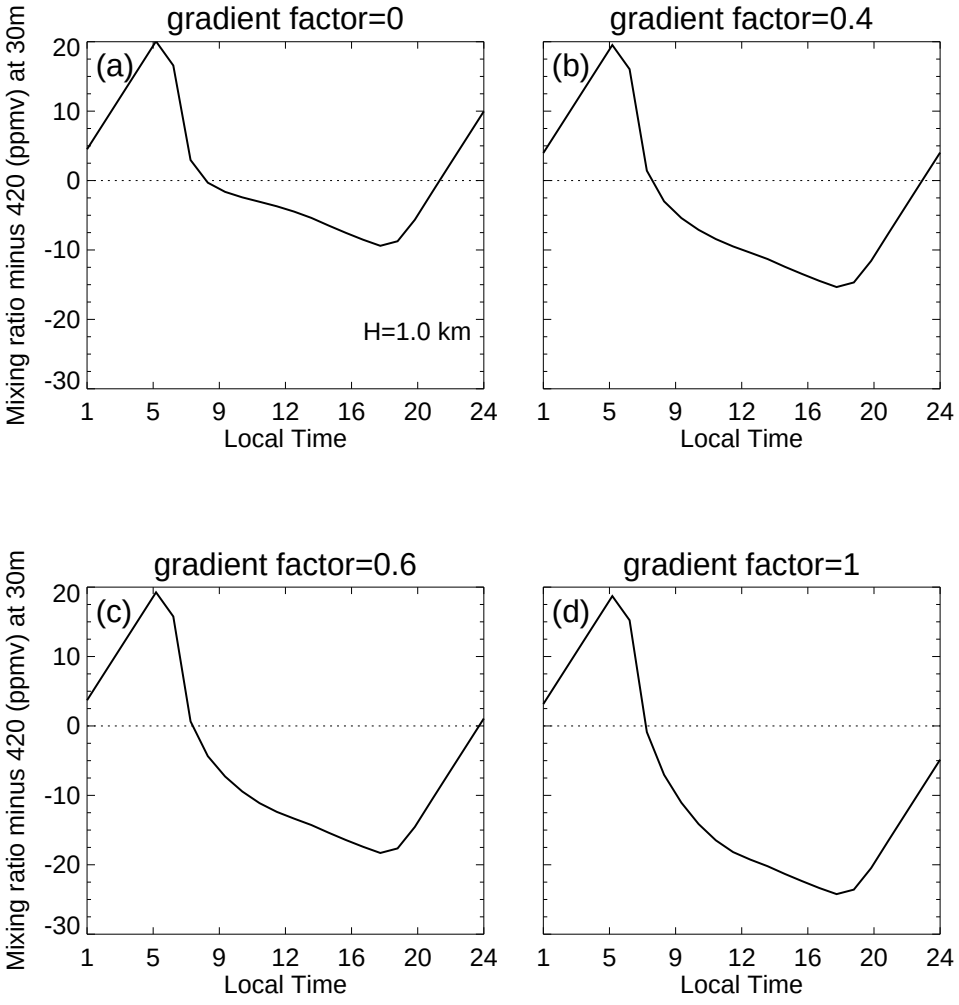

Figure 4. Diurnal variation of the benchmark mixing ratio at 30 m produced with the first kind of surface flux for $\alpha = 0$ (a), $\alpha = 0.2$, $\alpha = 0.6$ (c) and $\alpha = 1$ (d).

the unstable condition, it affects E mostly during daytime during which the vertical gradient of chemical tracers is weak due to strong mixing. The weak gradient can dampen the impact of the ABL-H according to Eq. (2.10).

To examine the impact of the ABL-H on diffusion coefficient we consider the following perturbed TKE equation due to the change of the ABL-H

https://doi.org/10.5194/acp-2023-37
Preprint. Discussion started: 7 February 2023

Atmospheric Chemistry and Physics Discussions

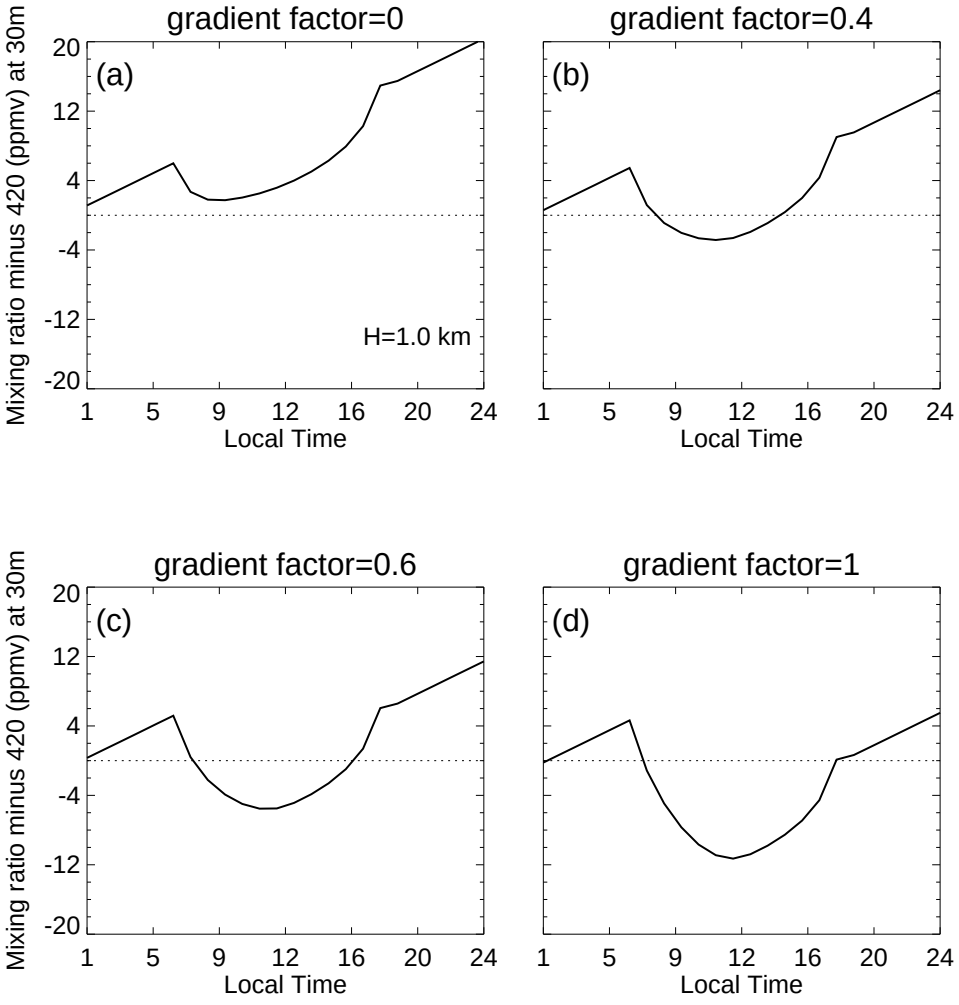

Figure 5. Same as Fig.4 but with the second kind of emission scheme.

$$\frac{\partial \delta E}{\partial t} = \alpha(z,t)\delta E + \frac{\partial}{\partial z}\left(\beta(z,t)\delta E + K_M \frac{\partial \delta E}{\partial z}\right), \tag{3.4}$$

where

$$\alpha = \frac{B}{2\sqrt{E}} - \frac{3}{2}C\sqrt{E}, \quad \beta = \frac{c\lambda}{2\phi_m\sqrt{E}}\frac{\partial E}{\partial z}. \tag{3.5}$$

https://doi.org/10.5194/acp-2023-37
Preprint. Discussion started: 7 February 2023

Atmospheric Chemistry and Physics Discussions

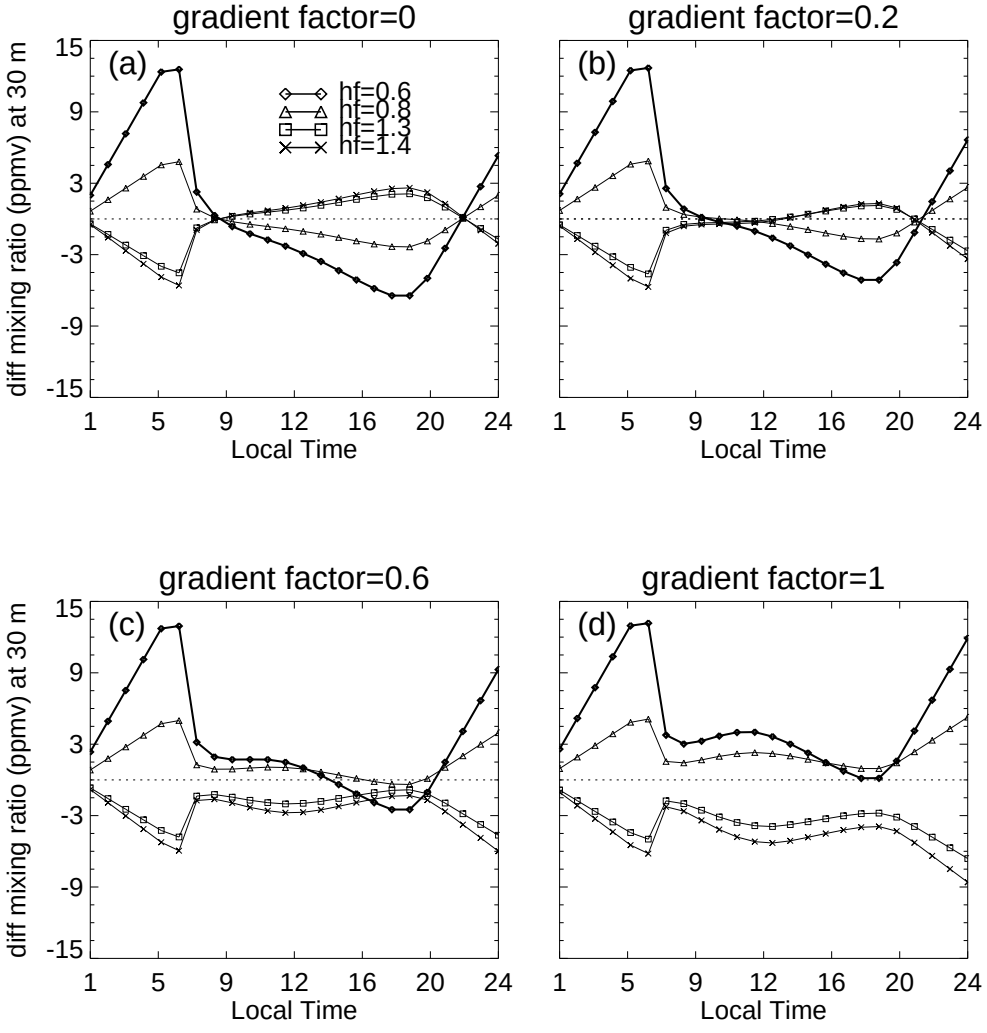

Figure 6. Differences between the benchmark mixing ratio and mixing ratios with hf =0.6, 0.8, 1.3, 1.4 for $\alpha = 0$ (a), $\alpha = 0.2$, $\alpha = 0.6$ (c), and $\alpha = 1$ (d) at 30 m. The first kind of surface flux is used in the calculation.

Lower boundary condition for δE is

$$\delta E(z=0,t) = \begin{cases} 0 & \text{stable} \\ \frac{0.4}{3}\frac{w_*^2}{h}\delta h \equiv \kappa \delta h & \text{unstable.} \end{cases} \tag{3.6}$$

https://doi.org/10.5194/acp-2023-37
Preprint. Discussion started: 7 February 2023

Atmospheric Chemistry and Physics Discussions

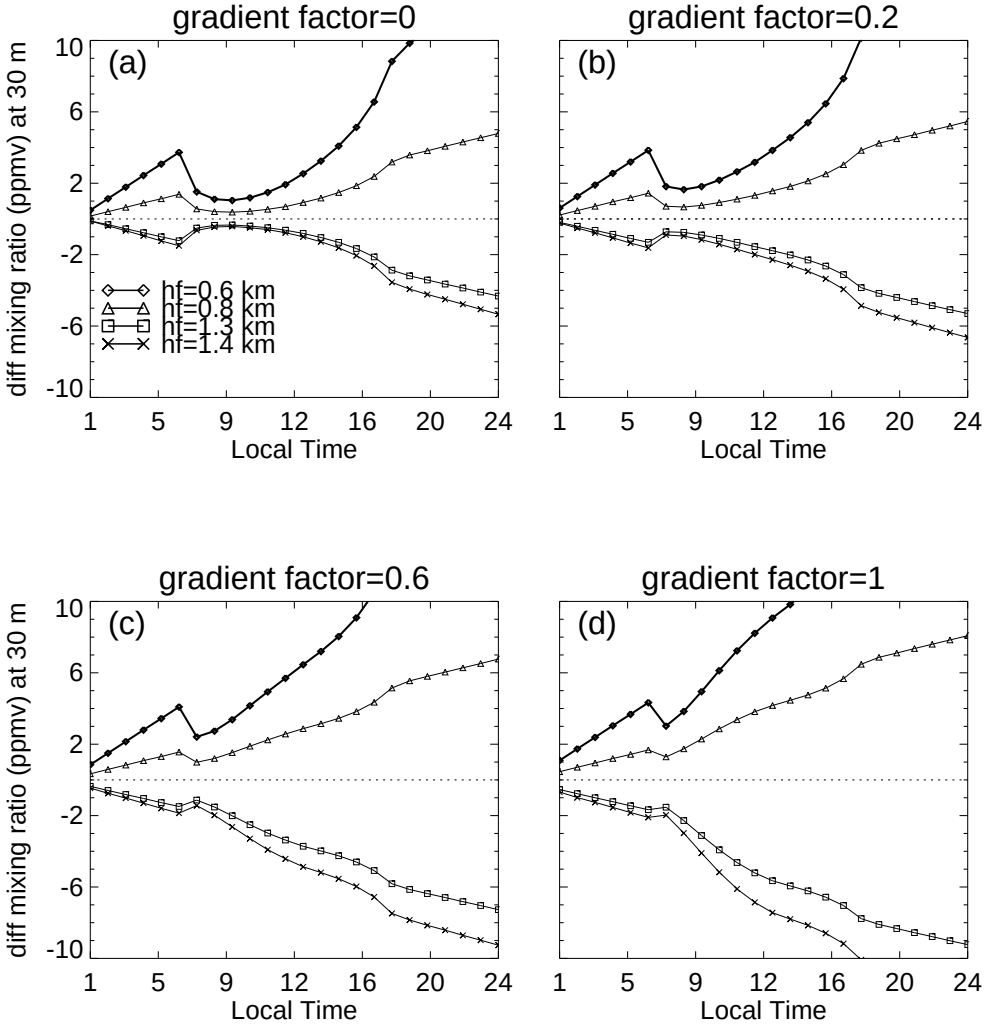

Figure 7. Same as Fig.6 but with the second kind of surface flux.

Analytical solution of Eq. (3.6) cannot be obtained in general. Here we consider the special case in which α, β, K_M are constants. In this special case the change of K_M corresponding change of the ABL-H is (Appendix)

$$\delta K_M = \frac{c\lambda}{4\phi_m\sqrt{E}} \int_0^t \frac{\kappa(\tau)\delta h(\tau) K_M}{\sqrt{\pi(t-\tau)^3}} \exp\left[-\left(\Lambda + \frac{K_M^2}{4(t-\tau)}\right) z\right] d\tau \tag{3.7}$$

https://doi.org/10.5194/acp-2023-37
Preprint. Discussion started: 7 February 2023

Atmospheric Chemistry and Physics Discussions

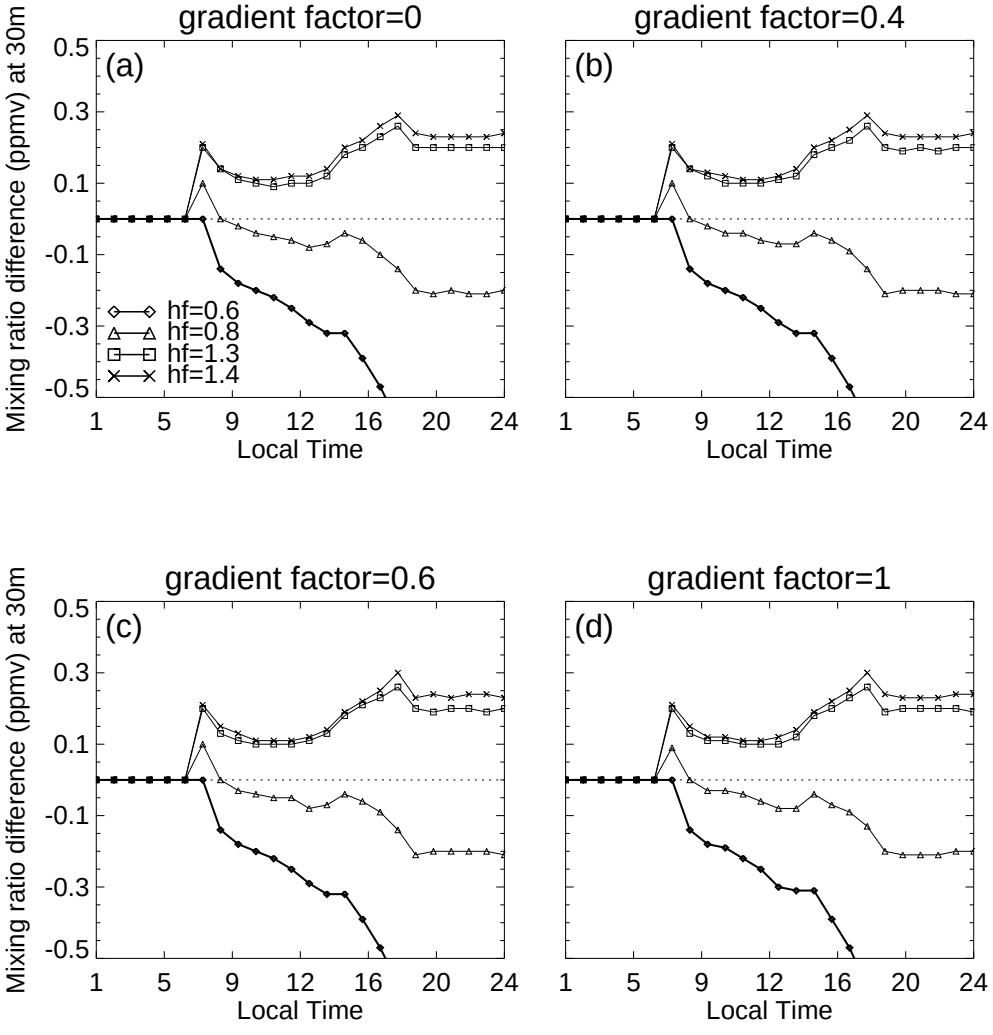

Figure 8. Difference between the mixing ratio with $\gamma_\psi \neq 0$ and mixing ratio with $\gamma_\psi = 0$ at 30 m with hf =0.6, 0.8, 1.3, 1.4 and the first kind of surface flux for α =0 (a), α =0.4 (b), α =0.6 (c) and α =1 (d).

where Λ is defined in (B.4). (3.7) shows that the change of K_M is proportional to δh and decays as as height increases.

https://doi.org/10.5194/acp-2023-37
Preprint. Discussion started: 7 February 2023

Atmospheric Chemistry and Physics Discussions

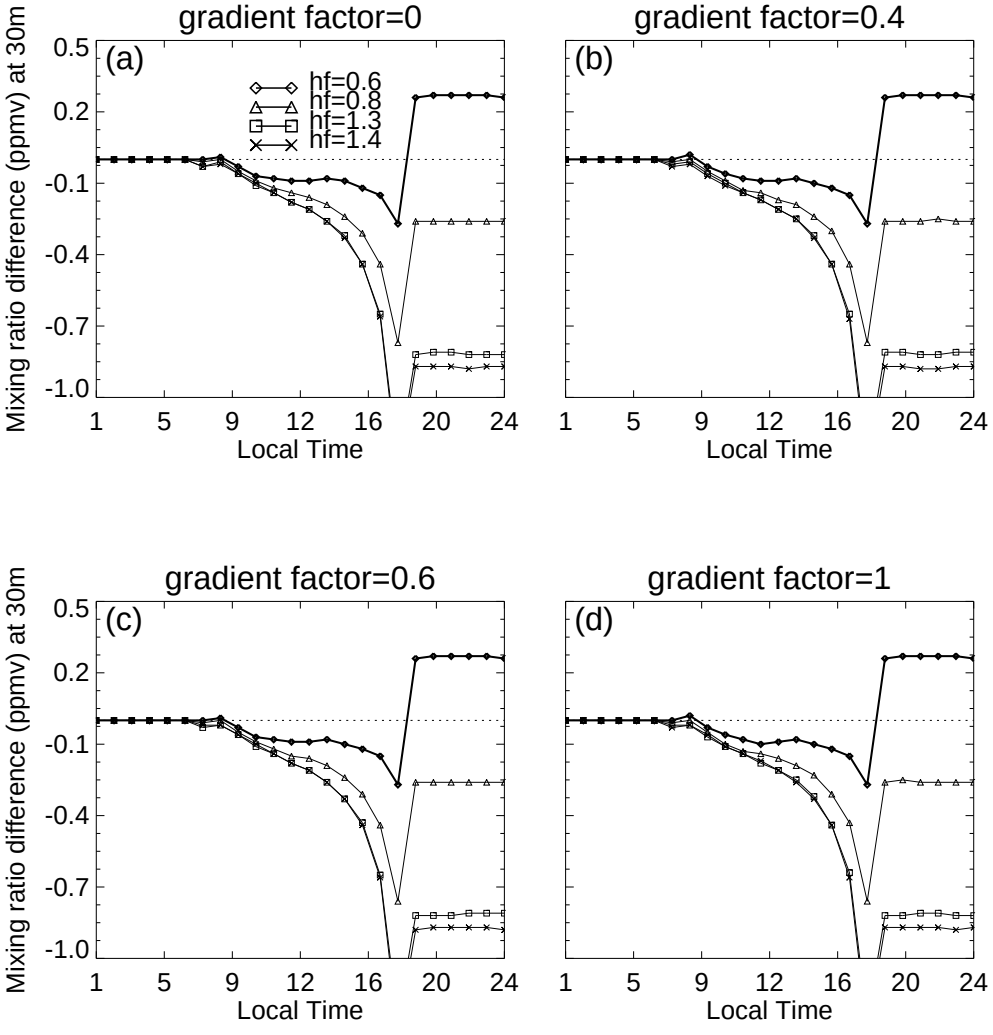

Figure 9. Same as Fig.8 but with the second kind of surface flux.

https://doi.org/10.5194/acp-2023-37
Preprint. Discussion started: 7 February 2023

Atmospheric Chemistry and Physics Discussions

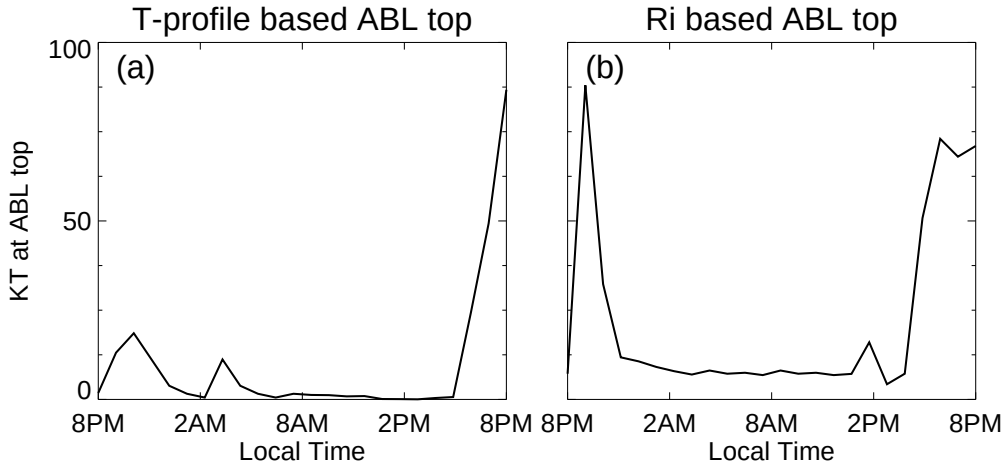

Figure 10. K_T at the top of the ABL over urban center of Toronto for the temperature gradient based ABL-H definition (a), and for the Richardson number based definition (b).

3.2 Impacts of the ABL-H in GEM-MACH

The analyses in section 3.1 are based on the constant coefficient assumption. To examine the impact of the ABL-H on chemical species in more realistic meteorological and chemical environment, numerical models with the TKE-based scheme should be employed. GEM-MACH is a multi-scale chemical weather forecast model developed by Environment and Climate Change Canada. It is composed of dynamics, physics, and on-line chemistry and transport modules. Because GEM-MACH uses the TKE parameterization scheme, it is an ideal tool to examine the impacts of the ABL-H. In the model, the ABL-H affects the vertical diffusion coefficient through the convective velocity and initial TKE. It is also involved in the computation of the boundary layer sub-grid-scale cloud properties, mixing length when the Blackadar's formulation is used and the computation of the plume rise.

Two approaches can be used to examine the impact of the ABL-H on the concentration in GEM-MACH simulation. In the first approach the impact is examined based on the correlation during different time period between the ABL-H and

https://doi.org/10.5194/acp-2023-37
Preprint. Discussion started: 7 February 2023

Atmospheric Chemistry and Physics Discussions

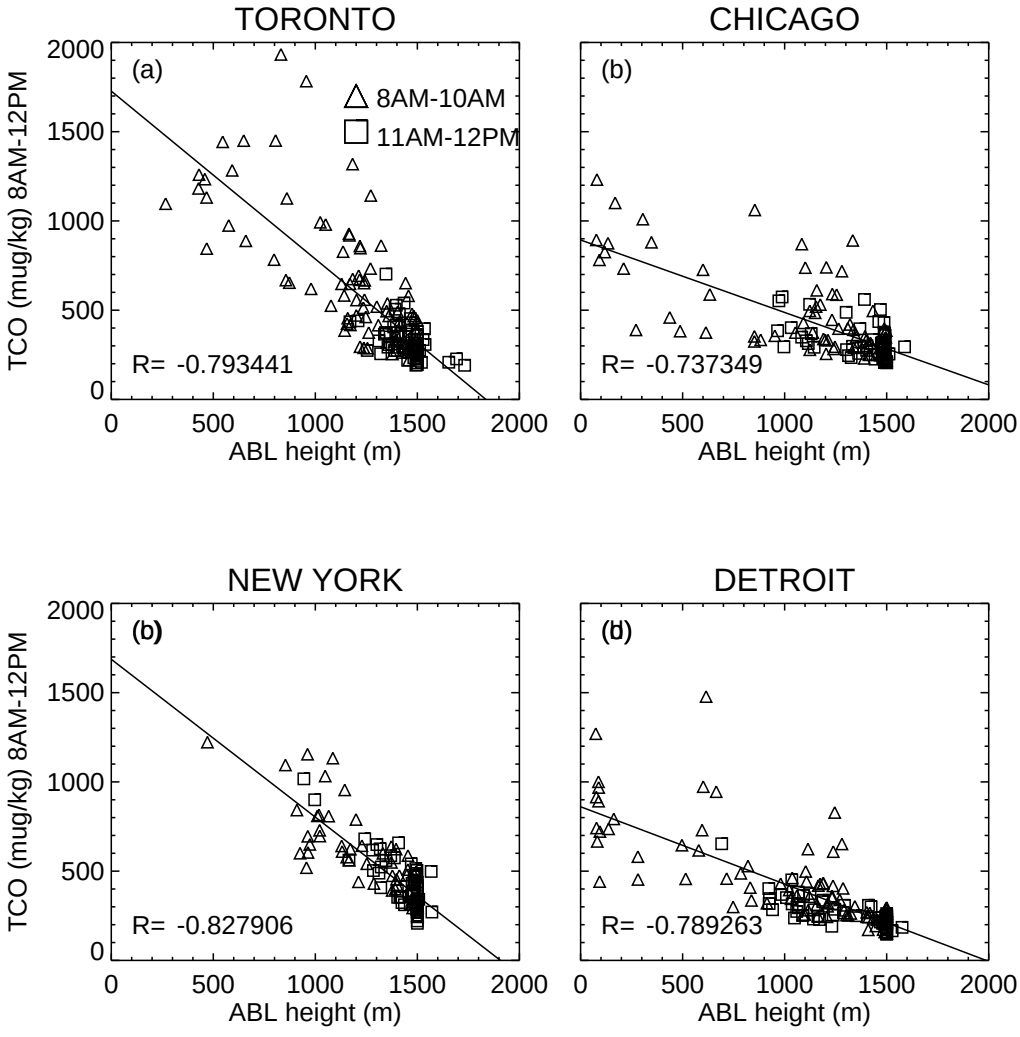

Figure 11. Scatter plot of the area mean CO mixing ratio and the temperature profile based ABL-H over Toronto (a), Chicago (b), New York City (c) and Detroit (d). Triangles and squares represent data between 8:00AM to 10:00AM, and between 11:00AM to 12:00PM in July 2015, respectively.

https://doi.org/10.5194/acp-2023-37
Preprint. Discussion started: 7 February 2023

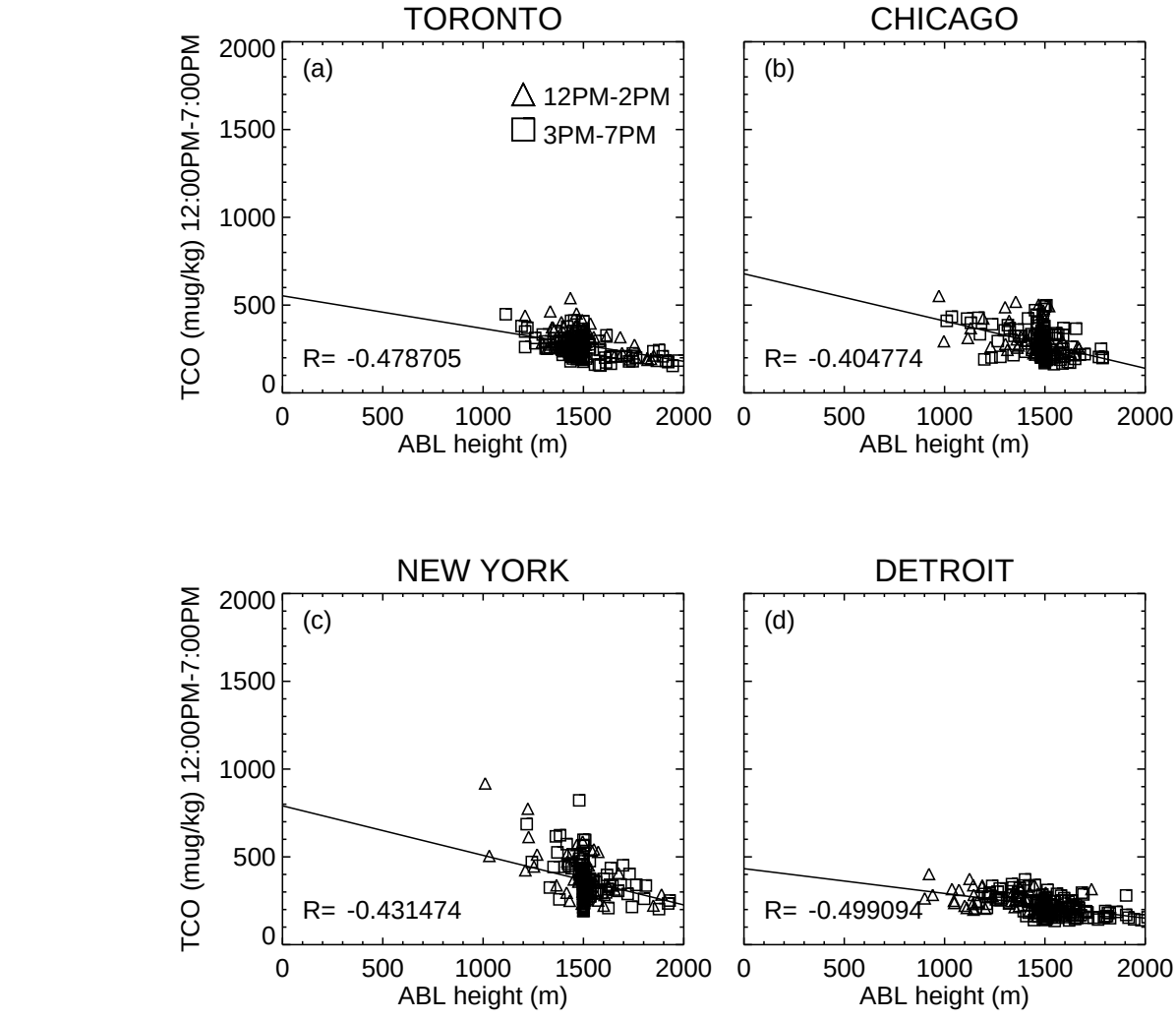

Figure 12. Same as Fig. 11 but for 12:00PM to 7:00PM. Triangles and squares represent data between 12:00PM to 2:00PM, and between 3:00PM to 7:00PM, respectively.

concentration calculated with model simulation results. Because other processes are involved in the simulation, the correlation is not entirely associated with the impact of the ABL. In the second approach the impact is investigated based on the sensitivity

https://doi.org/10.5194/acp-2023-37
Preprint. Discussion started: 7 February 2023

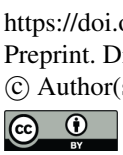

Atmospheric Chemistry and Physics Discussions

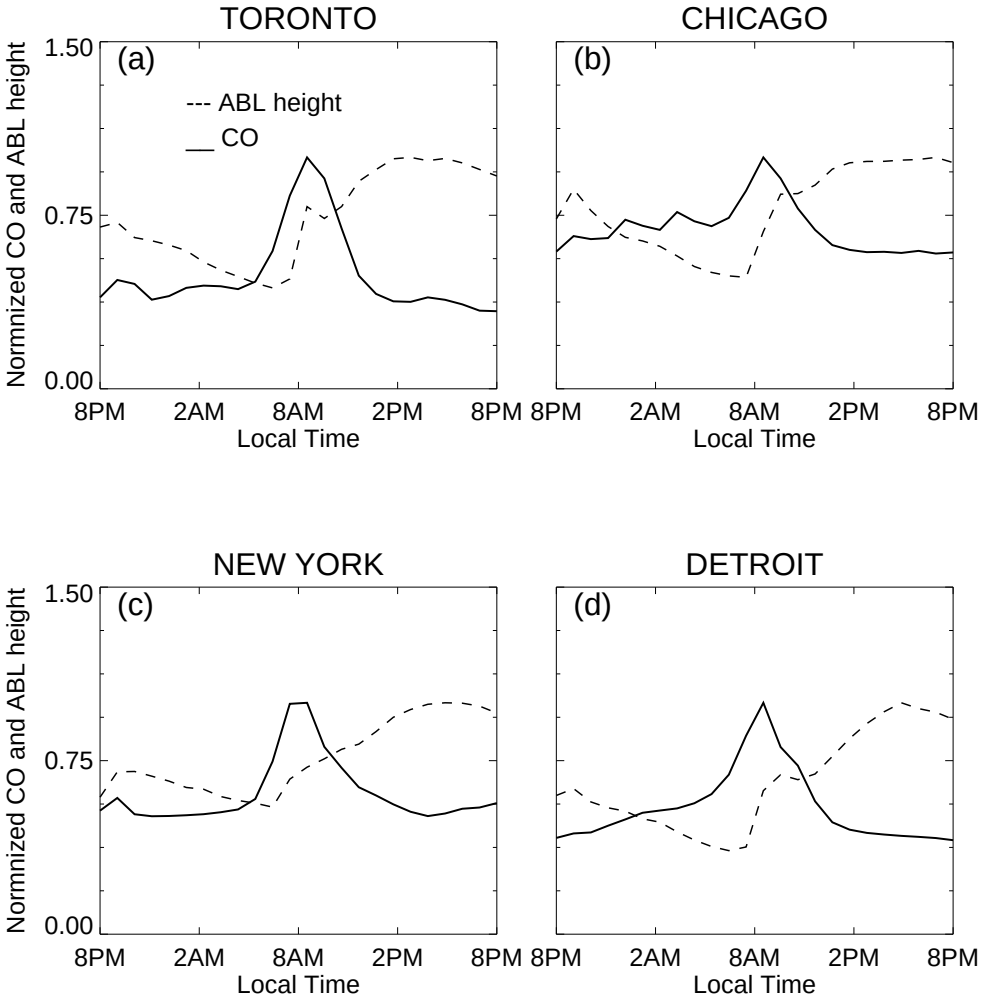

Figure 13. Diurnal variation of the normalized average of CO mixing ratio (solid lines) and the ABL-H (dashed lines) over Toronto (a), Chicago (b), New York City (c) and Detroit (d).

225 results. Since the differences of concentrations between the sensitivity tests and the benchmark simulation are entirely due to the change of the ABL-H, this approach can help better understand the impact of the ABL-H on the concentration of chemical species in model simulations.

In the following part, the two approaches are used to examine the impact of the ABL-H. To see the impacts of different ABL-H definition on the correlation and sensitivity results, two versions of GEM-MACH are used in this section. In the first

https://doi.org/10.5194/acp-2023-37
Preprint. Discussion started: 7 February 2023


Atmospheric Chemistry and Physics Discussions

version, the ABL-H is computed based on the vertical profile of temperature, and based on the Richardson number in the second version. In addition to the difference in the ABL-H, there are other differences in the two versions.

3.2.1 Correlation between CO concentration and the ABL-H

Because both vertical diffusivity and the ABL-H are affected by the surface heat flux, concentration of chemical species and the ABL-H should have different correlation at different time period. In this part, the mean values of the ABL-H and CO over the urban center of Toronto, Chicago, New York City and Detroit are computed using the model simulation results in July 2015. The results are then used to compute the correlations between the ABL-H and CO over 8:00AM to 12:AM and over 12:00PM to 7:00PM are examined based on simulation results with the two GEM-MACH versions.

3.2.2 Correlation simulated with the first GEM-MACH version

Figure 11. is a scatter plot showing the correlation between the area mean CO mixing ratio at the lowest model level (about 22 m above the ground in Toronto) and the area mean ABL-H during 8:00AM to 12:00PM in July 2015 over the four urban areas. In the figure, there is a strong negative correlation over the four urban centers. Variation of the correlation in the four urban centers is small: New York City has the strongest correlation (-0.83) and Chicago has the weakest correlation (-0.74). The figure also shows that the correlation over 8:00AM to 10:00AM is different from correlation over 10:00AM to 12:00PM. In the afternoon, correlation shown in Fig. 12 is much weaker than the correlation in the morning, particularly after 2:00PM. The magnitude of the correlation is about half of that in the morning. Like the correlation in the morning, the variation of correlation over the four areas is small with the strongest correlation over Detroit (-0.5) and the weakest correlation over Chicago (-0.4). The correlations between the ABL-H and NO_2 are similar (not shown).

The correlation can be seen more clearly by comparing the diurnal variation of the normalized averaged mixing ratio of CO and the ABL-H (by their maximum) over the four urban centers shown in fig. 13. It can be seen from the figure that the correlation between 7:00AM and 8:00AM is positive due to the sudden jump of surface heat flux at sunrise, and is negative in other time. The negative correlation is strong between 8:00AM and 2:00PM and is weak in other time.

3.2.3 Correlation simulated with the second GEM-MACH version

To see the simulated correlation between CO and the Richardson-number-based ABL-H, the second version of GEM-MACH is employed to simulate CO field and the ABL-H. Figs 14 and 15 show the correlation of the area mean CO mixing ratio and ABL-H over 8:00AM to 12:PM and over 12:PM to 7:00PM in July 2015, respectively. Negative correlations over 8:00AM to 12:PM are much weaker than those simulated with the first version of GEM-MACH (Fig.11) The variation of the correlation over the four areas is large with -0.54 over Detroit and -0.19 over Chicago. The correlation in the afternoon (Fig. 15) is similar in magnitude and variation. The weak correlation is associated with the lower values of mixing ratio and the ABL-H produced by the second version of GEM-MACH (not shown). reflect the impact of different ABL-H definition on chemical tracers.

https://doi.org/10.5194/acp-2023-37
Preprint. Discussion started: 7 February 2023

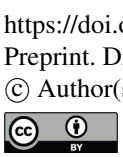

Atmospheric Chemistry and Physics Discussions

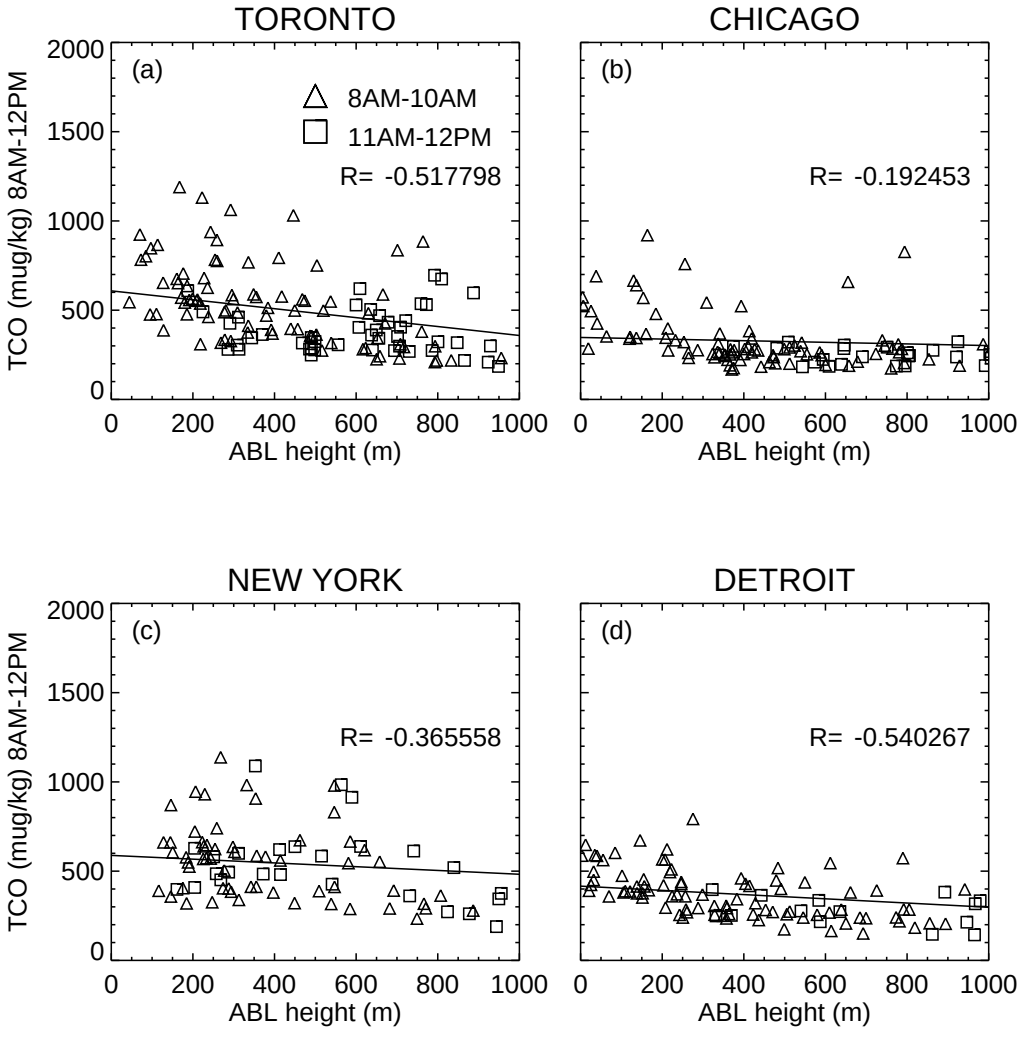

Figure 14. Same as Fig. 11 but for the Richardson number based ABL-H.

https://doi.org/10.5194/acp-2023-37
Preprint. Discussion started: 7 February 2023

Atmospheric Chemistry and Physics Discussions

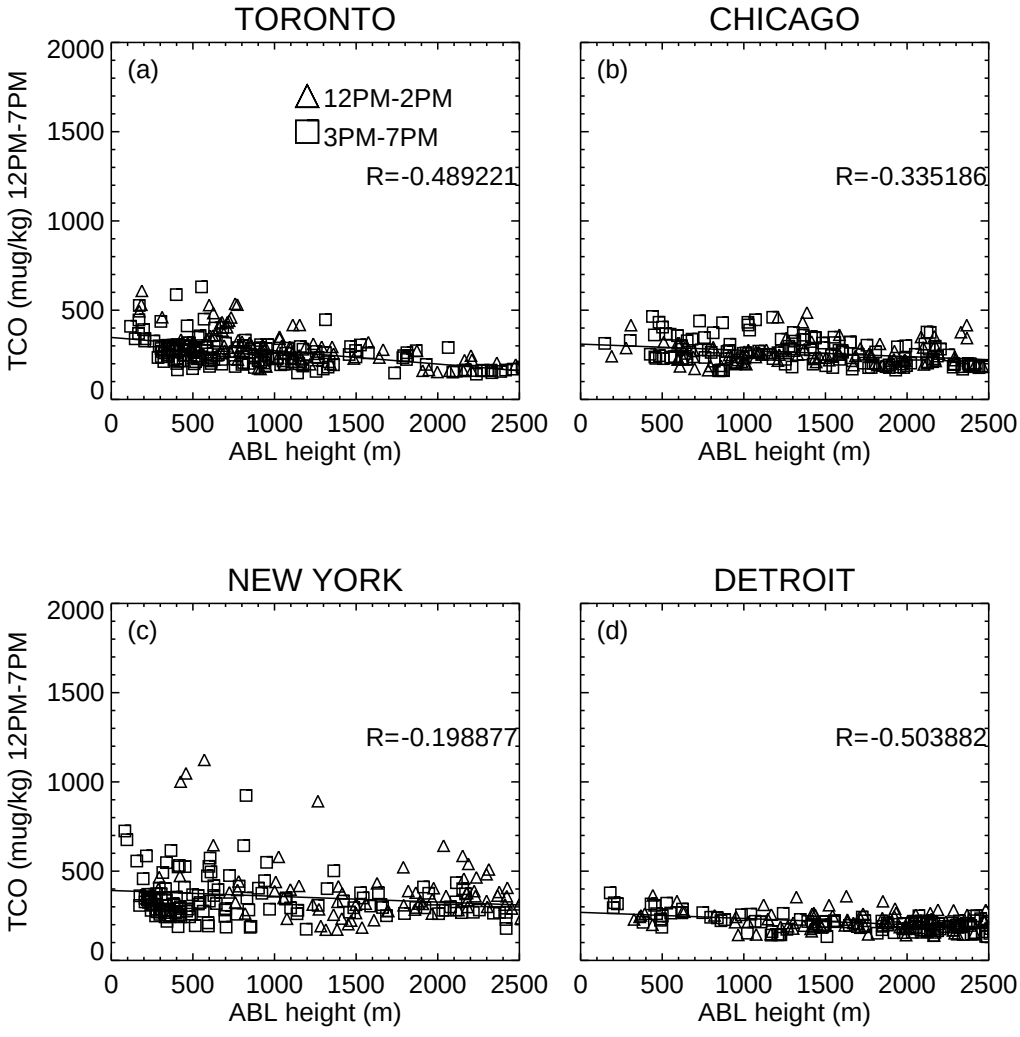

Figure 15. Same as Fig. 12, but for the Richardson number based ABL-H.

3.2.4 Sensitivity tests

Because concentration of chemical species and the ABL-H are both under the influence of diurnal variation of vertical diffusivity, correlations shown above reflect only part of the effect of the ABL-H on chemical species. In this part, the sensitivity of chemical species to the change of ABL-H is examined based on simulation results with different ABL-H.

https://doi.org/10.5194/acp-2023-37
Preprint. Discussion started: 7 February 2023

Atmospheric Chemistry and Physics Discussions

3.2.5 Sensitivity tests with the first GEM-MACH version

The impacts of the ABL-H on chemical species can be examined by the sensitivity test. In this part, four scenario simulations with hf =0.8, 1, 1.2 and 1.4 representing the under- and over-estimated ABL-H scenarios are carried out. Since the ABL-H affects concentration of chemical species through diffusivity which are associated with TKE and the convective velocity, the impacts of the ABL-H on the diurnal variations these variables are investigated by comparing the benchmark GEM-MACH simulation (with hf =1) against the three scenario simulations.

The numerical results show that the maximum differences of w^* between the scenario and benchmark simulations appear at around 2:00PM (not shown). The monthly mean diurnal variations of the corresponding TKE differences at the lowest model level over the four urban centers are shown in Fig. 16. It can be seen from the figure that the pattern of the diurnal variation over the four urban centers are similar. Increase of the ABL-H leads to the increase of TKE, and the differences reach a maximum at 2:00PM. The magnitude of the difference is roughly proportional to the magnitude of the ABL-H difference. The change of TKE at higher model levels are smaller than those at the lowest model level (not shown). All these features agree with the analytical results.

In GEM-MACH, the averaged diffusion coefficient over the last two model levels is used in computing the concentration of chemical species at the last model level. The differences of the averaged coefficient of the two levels between the scenario simulations and benchmark simulation are shown in Fig. 17. The comparison between Fig. 16 and Fig. 17 shows that the diffusion coefficient and TKE differences have a very strong positive correlation.

The impact of the ABL-H on the mixing ratio of CO can be seen from Fig. 18 which shows the mixing ratio differences between the scenario simulations and the benchmark simulation. The impacts over the urban centers of Chicago and Detroit are very small. Over the urban center of Toronto, large ABL-H leads to reduction of CO concentration after 2:00PM. However that is not the case over urban center of New York City where decrease of the ABL-H leads to small concentration right before 2:00PM and the increase of the ABL-H leads to increase of concentration after 2:00PM. The maximum impact is about 15μg/kg which is about 5% of benchmark concentration. The impact of the ABL-H on NO_2 has a similar evolution pattern to that but with a larger magnitude (not shown).

In the early morning, the change of the ABL-H has very small impact on CO but noticeable impact on NO_2. Increase/decrease of the ABL-H does not always lead to decrease/increase of both CO and NO_2 concentration.

3.2.6 Sensitivity tests with Richardson number based ABL-H

Results in section 3.1 show that the ABL-H with different definition has different correlation with chemical species. To see how the different definition changes the sensitivity results, the second version of GEM-MACH is used to simulate the concentration of species with different ABL-H. Figure 19 shows that the sensitivity of diffusion coefficient to the change of the ABL-H is similar to that shown in Fig.17: a large/small ABL-H leads to a large/small diffusion coefficient. The comparison between Fig. 17 and 19 suggests that in both cases the impacts of the ABL-H are very small over Chicago and Detroit, and have similar order of magnitude over Toronto and New York City. As with the results with the first version of GEM-MACH , the change

https://doi.org/10.5194/acp-2023-37
Preprint. Discussion started: 7 February 2023

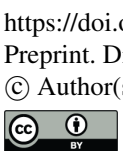

Atmospheric Chemistry and Physics Discussions

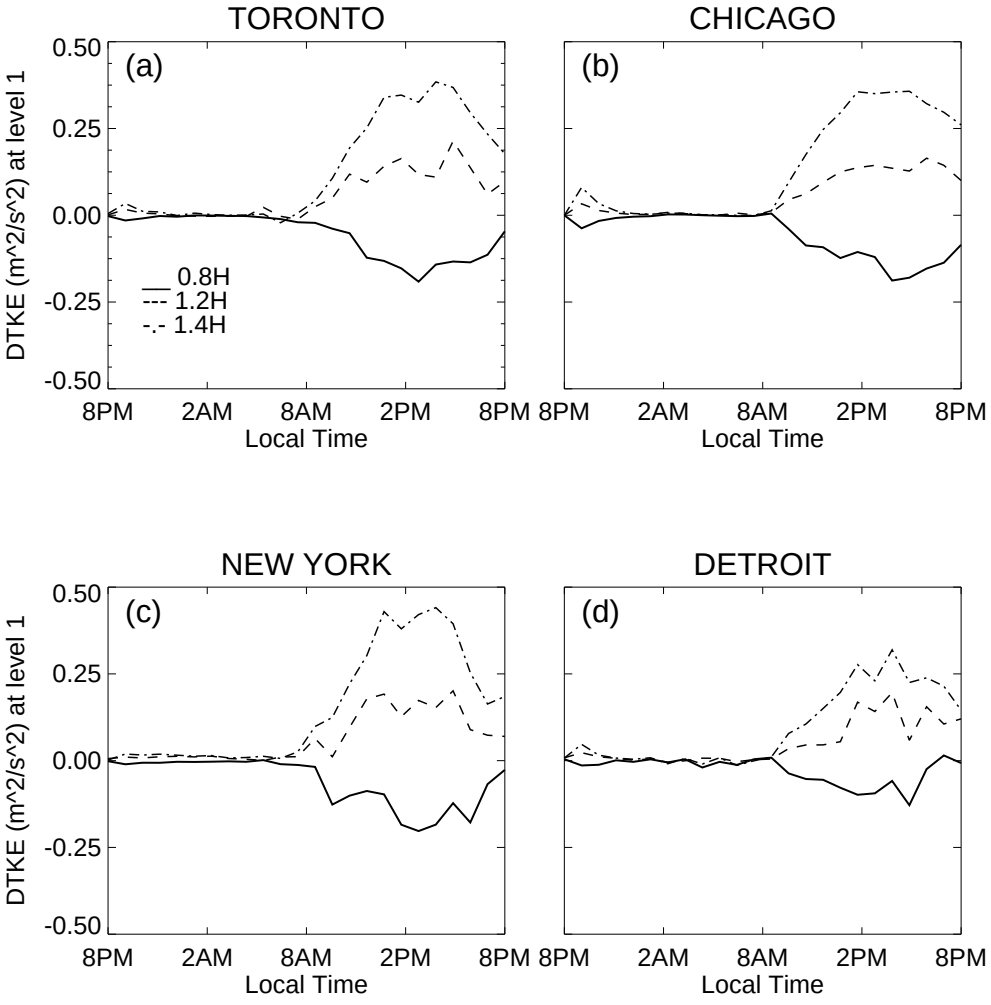

Figure 16. Diurnal variation of the monthly mean TKE differences at the lowest model level between the three scenario simulations and benchmark simulations with the temperature profile based ABL-H over Toronto (a), Chicago (b), New York City (c) and Detroit (d).

of the ABL-H in the early morning has very small impact on concentration of CO, and the increase/decrease does not always leads to decrease/increase of CO concentration (Fig. 20).

The sensitivity test results with the two GEM-MACH versions show that a large/small diffusion coefficient does not always lead to a small/large concentration of chemical species. This is very different from the sensitivity results with the K-profile scheme in which the increase/decrease of the ABL-H always leads to the decrease/increase of tracer's concentration for negative

https://doi.org/10.5194/acp-2023-37
Preprint. Discussion started: 7 February 2023

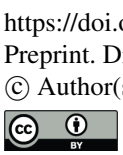

Atmospheric Chemistry and Physics Discussions

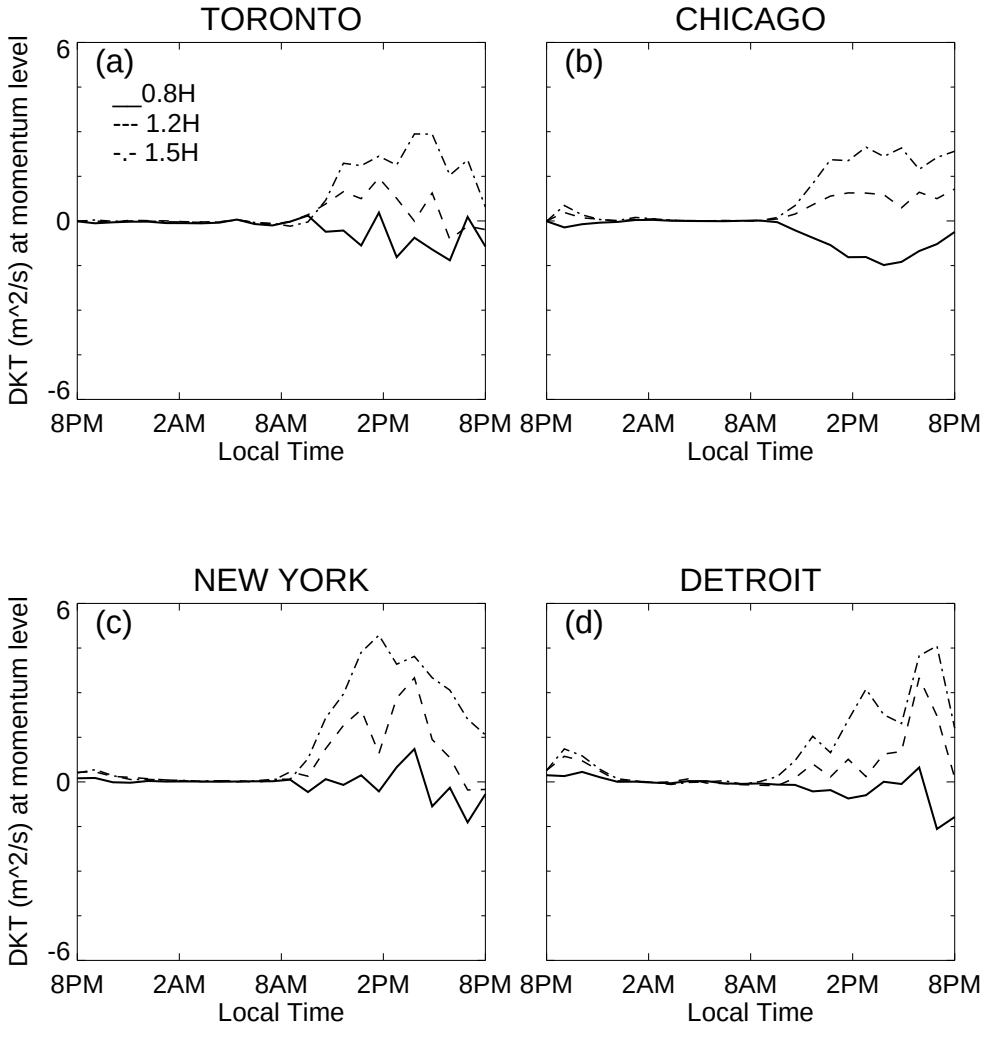

Figure 17. Diurnal variation of the monthly mean diffusivity differences averaged over the two lowest model levels between the three scenario simulations and benchmark simulations with the temperature profile based ABL-H over Toronto (a), Chicago (b), New York City (c) and Detroit (d).

https://doi.org/10.5194/acp-2023-37
Preprint. Discussion started: 7 February 2023

Atmospheric Chemistry and Physics Discussions

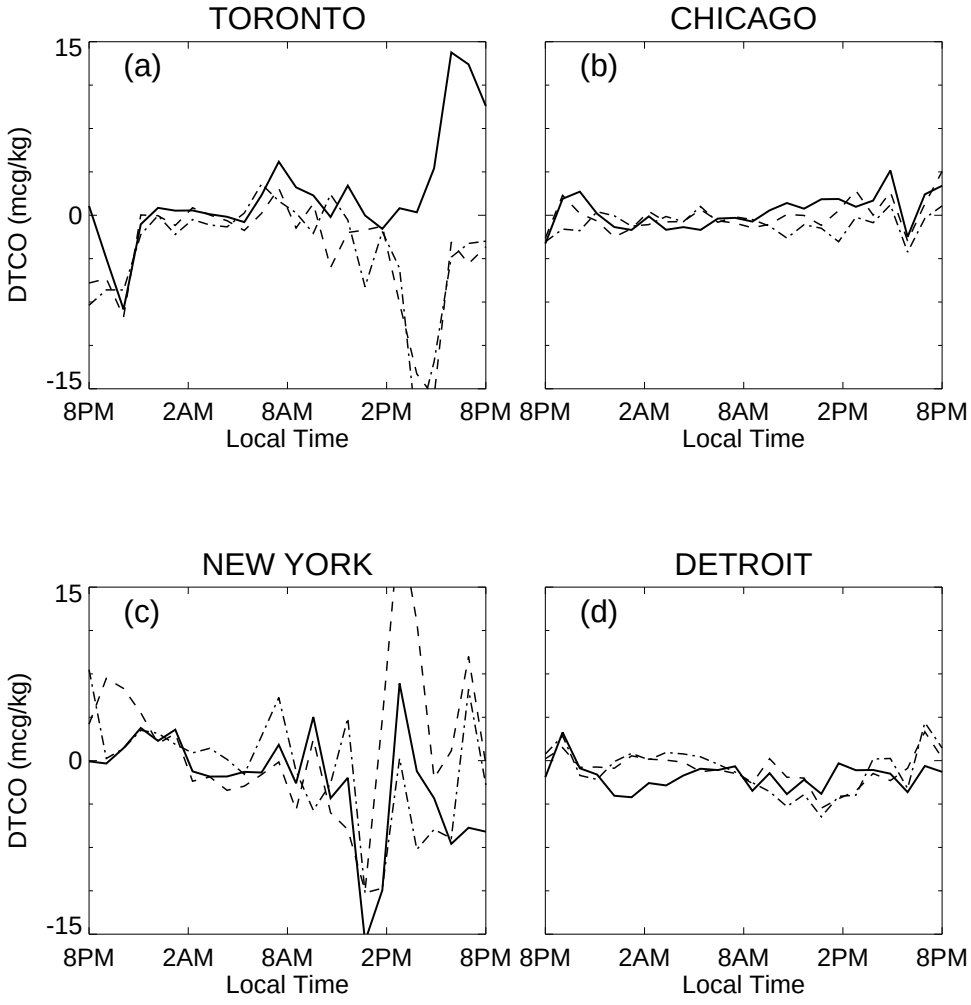

Figure 18. Diurnal variation of the monthly mean differences of the mixing ratio of CO at the lowest model level between the three scenario simulations and benchmark simulations over Toronto (a), Chicago (b), New York City City (c) and Detroit (d).

vertical gradient of tracer. Weak sensitivities suggest that the uncertainties in the ABL-H would have limited impact on the prediction of the chemical species with GEM-MACH.

https://doi.org/10.5194/acp-2023-37
Preprint. Discussion started: 7 February 2023

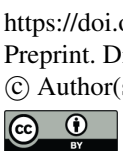

Atmospheric Chemistry and Physics Discussions

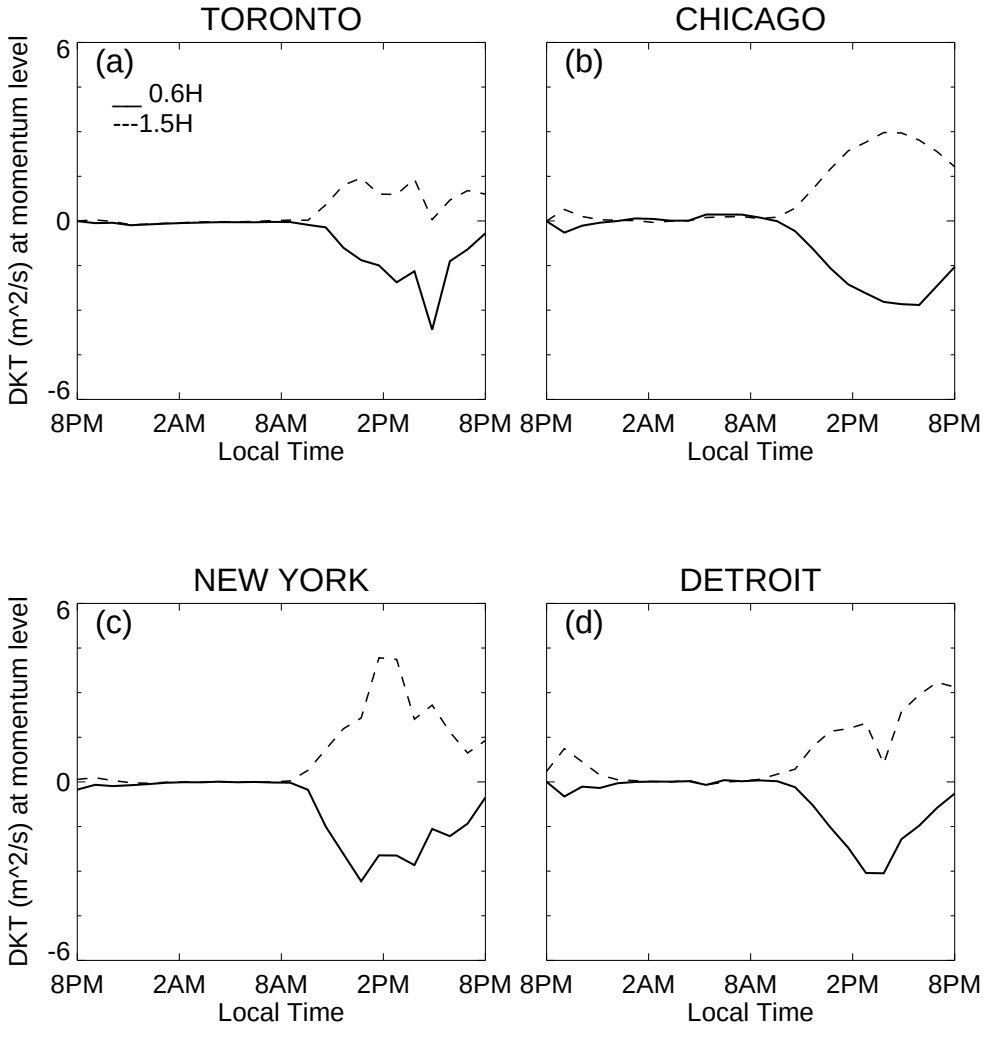

Figure 19. Diurnal variation of the monthly mean diffusion coefficient differences at the lowest model level between the three scenario simulations and benchmark simulations with the Richardson number based ABL-H over Toronto (a), Chicago (b), New York City (c) and Detroit (d).

https://doi.org/10.5194/acp-2023-37
Preprint. Discussion started: 7 February 2023

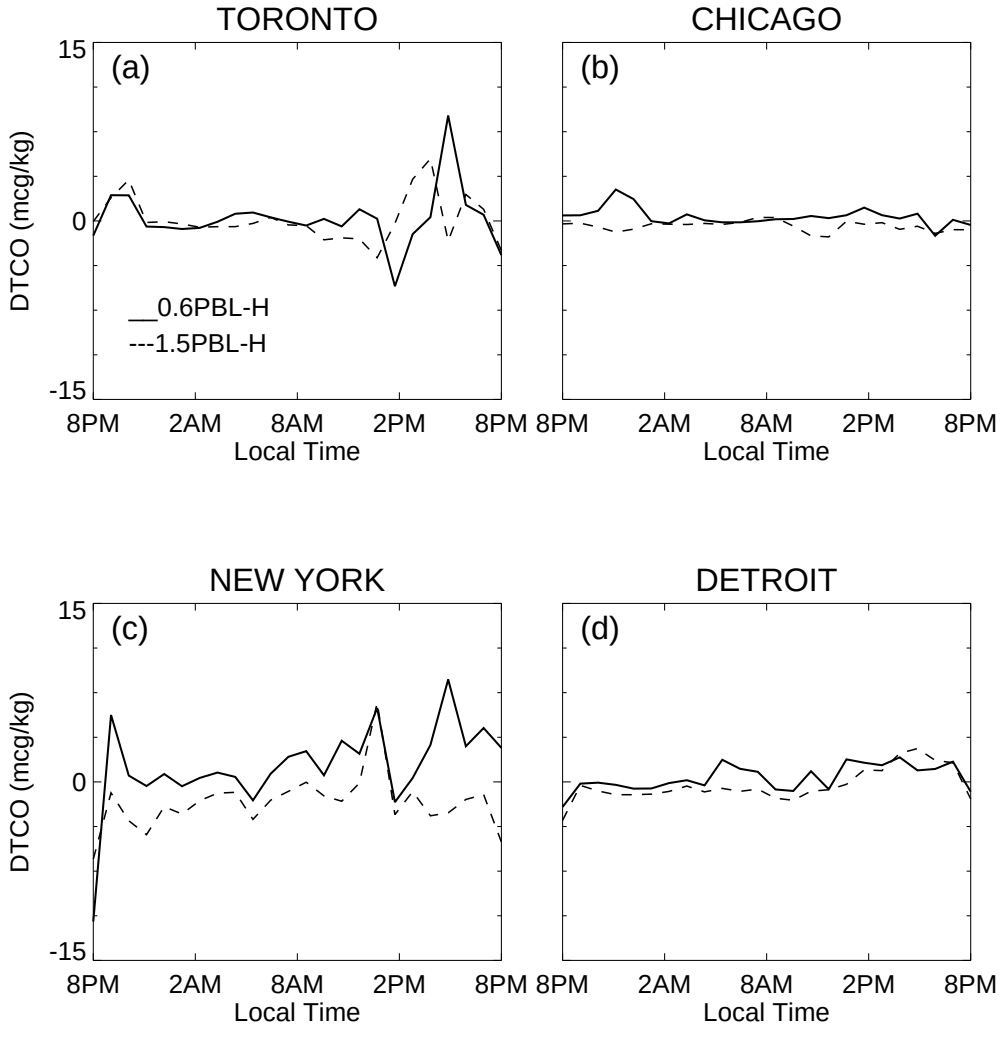

Figure 20. Diurnal variation of the monthly mean differences of the mixing ratio of CO at the lowest model level between the three scenario simulations and benchmark simulations with the Richardson number based ABL-H over Toronto (a), Chicago (b), New York City City (c) and Detroit (d).

https://doi.org/10.5194/acp-2023-37
Preprint. Discussion started: 7 February 2023

Atmospheric Chemistry and Physics Discussions

4 Summary and discussion

The ABL-H is involved in the ABL parameterization scheme employed in numerical models. It affects the concentration of chemical species within the ABL by changing the vertical diffusivity and the volume of tracer in the ABL. Due to uncertainties in meteorological fields and different definitions of the ABL-H there exists large uncertainties in the ABL-H. Their impacts on the simulation of concentration of chemical species are examined by using K-profile and TKE-based parameterization schemes.

In the K-profile scheme, the ABL-H is involved directly in the calculation of diffusion coefficient. The numerical results based on a 1-D diffusion model with the K-profile scheme show that in the early morning and nighttime, the increase/decrease of the ABL-H leads to decrease/increase of tracer's concentration by concentrating/diluting the air within the ABL. In an unstable ABL During the daytime, the sensitivity of the concentration of tracers to the ABL-H depends on not only the value of the ABL-H, but also on the surface flux and vertical gradient of tracers. For negative surface flux, large ABL-H leads to the increase of concentration if the (negative) gradient is weak, but leads to the decrease of concentration if the gradient is strong. However, for positive surface flux, large ABL-H always leads to the decrease of concentration for negative gradient of tracers. The impact of the ABL-H through the counter-gradient term is small. All these sensitivity results agree with analytical results.

In the TKE-based scheme, the ABL-H is involved in the lower boundary condition for the TKE equation. Its impact on TKE decays as height increases. The simulation results with GEM-MACH show that the correlation between the concentration of CO (and NO_2) and the ABL-H is strong in the morning but weak in the afternoon for the temperature profile based ABL. However, It is weak in both morning and afternoon for the Richardson number based ABL-H.

The sensitivity tests with the two kinds of ABL-H show that large/small ABL-H leads to large/small TKE and diffusion coefficient. However the large/small diffusion coefficient does not always lead to small/large concentration of chemical species during the daytime. These impacts are much smaller than those shown in the 1-D diffusion model with the K-profile scheme although the change of diffusivity due to the change of ABL-H is larger than that in the 1-D case. In the early morning, the change of the ABL-H has very small impact on the concentration of chemical species. The sensitivity results suggest that uncertainties in the ABL-H would not lead to large uncertainties in the simulation of chemical species with GEM-MACH.

Although the increase/decrease of the ABL-H leads to the increase/decrease of vertical diffusivity in both K-profile and TKE schemes, the sensitivities of the concentration of chemical species to the change of the ABL-H simulated with the two schemes are different. With the K-profile scheme the concentration of chemical species decreases/increases as the ABL-H increases/decreases in the early morning and daytime for negative vertical gradient of chemical species. However, with the TKE-based scheme, the increase/decrease of the ABL-H does not lead to the consistent decrease/increase of the concentration of chemical specie. The magnitude of sensitivity is extremely small in the early morning and is much smaller than that with the K-profile scheme during the daytime even the sensitivity of vertical diffusivity is stronger.

These different sensitivities are unlikely attributed to the sensitivity of meteorological fields because the sensitivities of temperature and wind to the ABL-H are small in GEM-MACH (not show). One possible reason for the differences is that the Green functions in the 1-D and 3D models are different due to the lack of meteorological fields in the 1-D model. The differences would produce different sensitivity results according to Eq. (2.10). However, this assumption cannot be verified

https://doi.org/10.5194/acp-2023-37
Preprint. Discussion started: 7 February 2023

Atmospheric Chemistry and Physics Discussions

because G cannot be computed in general. An indirect way to verify the assumption would be to implement the K-profile scheme in GEM-MACH and compare the sensitivity tests with those based on the 1-D model. This is our future work.

Appendix A: TKE equation

The TKE is defined as $(\overline{u'^2+v'^2+w'^2})/2$.. The evolution of TKE is described by the following equation (Mailhot & Benoit, 1982)

$$\frac{\partial E}{\partial t} = S + F + T + D, \tag{A.1}$$

where

$$S = -\overline{u'w'}\frac{\partial \bar{u}}{\partial z} - \overline{v'w'}\frac{\partial \bar{v}}{\partial z}, \tag{A.2}$$

$$F = \overline{w'b'}, \tag{A.3}$$

$$T = \frac{\partial}{\partial z}\left(\overline{w'E'} + \frac{1}{\rho_0}\overline{w'p'}\right), \tag{A.4}$$

$$D = -\mu\overline{|\nabla \times \mathbf{u}|^2} \tag{A.5}$$

are shear production term, buoyancy flux term, transport and pressure work (redistribution term) and dissipation, respectively.

Observations show that S and D are dominate terms at nighttime. While S is positive, D is negative. Both decay rapidly with height and become very small at around 0.6H. During the daytime, S and D are also dominate terms below 0.2H. S decays rapidly with height and becomes positive at 0.3H. F is also positive below 0.8H and decays linearly with height. T is negative below 0.4H and positive above. Its value increases with height. Above 0.4H the magnitude of the four terms is within -0.5 to 0.5.

In the TKE scheme $F+S$ is parameterized as $BE^{1/2}$, where B can be positive or negative, D is parameterized as $-CE^{3/2}$, where C is positive, and T is parameterized as $\partial(K_M\partial E/\partial z)/\partial z$, where K_M is positive.

Appendix B: Solution of Eq.(3.6)

Applying the Laplacian transform to Eq.(3.6), one has

$$K_M\frac{d^2\psi}{dz^2} + \beta\frac{\partial\psi}{\partial z} - (p+\alpha)\psi = 0. \tag{B.1}$$

By letting $\psi = \phi\exp(-\beta z/2K_M)$ the above equation can be transformed into the following form

$$\frac{d^2\phi}{dz^2} - \frac{1}{K_M}\left(p+\alpha+\frac{\beta^2}{4K_M}\right)\phi = 0. \tag{B.2}$$

Using the boundary condition and applying inverse Laplacian transform one obtains

$$\delta E = \int_0^t \frac{\kappa(\tau)\delta h(\tau)K_M}{2\sqrt{\pi(t-\tau)^3}}\exp\left[-\left(\Lambda + \frac{K_M^2}{4(t-\tau)}\right)z\right]d\tau, \tag{B.3}$$

https://doi.org/10.5194/acp-2023-37
Preprint. Discussion started: 7 February 2023


Atmospheric Chemistry and Physics Discussions

where

$$\Lambda = \frac{\alpha + 0.5\beta}{K_M} + \frac{\beta^2}{4K_M^2}. \tag{B.4}$$

Author contributions. Conceptualization, S.R. and C.S.; methodology, S.R.; software, S.R.; writing original draft preparation, S.R.; writing.review and editing, S.R. and C.S.

Competing interests. No competing interests are present

Acknowledgements. Comments and suggetsions from Drs. Stephen Belair and Ayrton Zadra are greatly appreciated.

https://doi.org/10.5194/acp-2023-37
Preprint. Discussion started: 7 February 2023

Atmospheric Chemistry and Physics Discussions

References

de Arellano, J. V.-G., B. Gioli, F. Miglietta, H. J. J. Jonker, H. K. Baltink, R. W. A. Hutjes, and A. A. M. Holtslag: Entrainment process of carbon dioxide in the atmospheric boundary layer, J. Geophys. Res., 109, D18110, doi:10.1029/2004JD004725, 2004.

Benoit, R., J. Cote., and J. Mailhot: Inclusion of a TKE boundary layer parameterization in the Canadian regional finite-element model. Mon. Wea. Rev., 17, 1726-1750, 1989.

Belair, S., J. Mailhot, J.W. Strapp, and J.I. MacPherson: An examination of local versus nonlocal aspects of a TKE-based boundary-layer scheme in clear convective conditions. J. Appl. Meteor., 38, 1499-1518 1999.

Culf A. D.: An application on simple models to Sahelian convective boundary-layer growth. Bound.-Layer Meteor., 58, 1-18, 1992.

Culf A. D., Fisch G., Malhi, G, Y., and Nobre, C. A.: The influence of the atmospheric boundary layer on carbon dioxide concentrations over a tropical forest, Agric. For Meteorol., 85, 149-158, 1997.

Dang X., Lai C-T,Hollinger D. Y., Schauer A., Xiao J., Munger J. W., Owensby C. Ehleringer R.: Combining tower mixing ratio and community model data to estimate regional-scale net ecosystem carbon exchange by boundary layer inversion over four flux towers in the United States, J. Geophys. Res., 116, G03036, doi:10.1029/2010JG001554, 2011.

Denmead, O. T., Raupach M. R., Dunin F. X. cleugh H. A. Leuning R.: Boundary layer budgets for regional estimates of scalar fluxes, Global Change Biol., 2(3), 255-264, doi:10.1111/j.1365-2486.1996.tb00077.x, 1996.

Lee. J, J. Hong, K. Lee, J. Hong, E. Velasco, Y. Lim, J. Lee, K. Nam, J. Park: Ceilometer monitoring of boundary-layer height and its application in evaluating the dilution effect on air pollution. Bound-Layer. Meteorol., 172, 435-455, doi:10.1007/s10546-019-00452-5, 2019

Holtslag, A. A. M. and B. A. Boville: Local versus non-local boundary layer diffusion on a global climate model. J. Climate, 6, 1825-1842 1993.

Holtslag, A. A. M. and C. -H. Moeng: Eddy diffusivity and countergradient transport in the convective atmospheric boundary layer. J. Atmos. Sci., 48, 1690-1698, 1991.

Lorente P., Raquel, P. A. Jimeez, J. Dudhia , and J. P. Montavez : Evaluating and improving the impact of the atmospheric stability and orography on surface winds in the WRF model, Mon. Wea. Rev., 144, no. 7 2685-93. https://doi.org/10.1175/MWR D 15 0449.1, 2016

Mailhot , J. , and R. Benoit: A finite-element model of the atmospheric boundary layer suitable for use with numerical weather prediction models. J. Atmos. Sci., 39, 2249-2266, 1982.

Pino P., J. Arellano, W. Peters, J. Schroter, C. Heerwaarden, M. Krol: A conceptual framework to quantify the influence of convective boundary layer development on carbon dioxide mixing ratios. Atmospheric Chem. Phys., 12 2969-2985. doi:10.5194/acp-12-2969-2012, 2012.

Raupach, M. R.: Vegetation.atmosphere interaction in homogeneous and heterogeneous terrain: Some implications of mixed.layer dynamics, Vegetatio, 91(1-2), 105-120, doi:10.1007/BF00036051 1991.

Ren S: Solutions to the 3D transport equation and 1D diffusion equation for passive tracers in the atmospheric boundary layer and their applications. J. Atmos. Sci., 76, 2143-2169, 2019.

Ren, S., Stroud, C. A., Belair, S., Leroyer, S., Munoz-Alpizar, R., Moran, M., Zhang, J., Akingunola, A.: Makar impact of urbanization on the predictions of urban meteorology and pollutants over four major north American cities. Atmosphere, 11 (9), 969, 2020.

Ren S, Stroud C. A.: Sensitivity of temperature to the surface heat flux and diffusivity in the atmospheric boundary layer, Atmosphere, 11, 978, doi:10.3390/atmos11090978, 2020.

https://doi.org/10.5194/acp-2023-37
Preprint. Discussion started: 7 February 2023

Atmospheric Chemistry and Physics Discussions

Seidel D. J., C. O. Ao, K. Li: Estimating climatological planetary boundary layer heights from radiosonde observations: Comparison of methods and uncertainty analysis, J. Geophys. Res., 116, D16113, doi:10.1029/2009JD013680, 2010..

Seidel D. J., Y. Zhang, A. Beljaars, T. Golaz, A. R. Jacobson, B. Medeiros: Climatology of the planetary boundary layer over the continental United States and Europe, J. Geophys. Res., 117, D17106, doi:10.1029/2012JD018143, 2012.

Su T., Z. Li, Y. Zheng, Q. Luan, J. Gauo: Abnormally shallow boundary layer associated with severe air pollution during the COVID.19 lockdown in China, Geophys. Res. Lett., 47, e2020GL090041, https://doi.org/10.1029/2020GL090041, 2020

Tennekes, H.: A model for the dynamics of the inversion above a convective boundary layer, J. Atmos. Sci., 30, 558-567, 1973.

Xiang Y., T. Zhang, J. Liu, L. Lv, Y. Dong, Z. Chen: Atmosphere boundary layer height and its effect on air pollutants in Beijing during winter heavy pollution, Atmos. Res., 215, 305-316, 2019.